Vaccine 27 (2009) 3912–3920

Contents lists available at ScienceDirect

Vaccine

journal homepage: www.elsevier.com/locate/vaccine

Synthetic peptides coupled to the surface of liposomes effectively induce SARS coronavirus-specific cytotoxic T lymphocytes and viral clearance in HLA-A*0201 transgenic mice

Satoshi Ohno[a,b], Shunsuke Kohyama[a,b], Maiko Taneichi[c], Osamu Moriya[a], Hidenori Hayashi[b], Hiroshi Oda[d], Masahito Mori[d], Akiharu Kobayashi[d], Toshitaka Akatsuka[a], Tetsuya Uchida[c], Masanori Matsui[a,*]

[a] Department of Microbiology, Faculty of Medicine, Saitama Medical University, Moroyama-cho, Iruma-gun, Saitama 350-0495, Japan
[b] Department of Pathological Biochemistry, Faculty of Pharmaceutical Sciences, Josai University, Sakado-city, Saitama 350-0295, Japan
[c] Department of Safety Research on Blood and Biological Products, National Institute of Infectious Diseases, Musashimurayama-city, Tokyo 208-0011, Japan
[d] Drug Delivery System Development Division, Nippon Oil and Fat Corporation, Tokyo 150-6019, Japan

ARTICLE INFO

Article history:
Received 19 September 2008
Received in revised form 5 March 2009
Accepted 2 April 2009
Available online 23 April 2009

Keywords:
SARS coronavirus
Liposomal peptides
Cytotoxic T lymphocytes

ABSTRACT

We investigated whether the surface-linked liposomal peptide was applicable to a vaccine based on cytotoxic T lymphocytes (CTLs) against severe acute respiratory syndrome (SARS) coronavirus (SARS-CoV). We first identified four HLA-A*0201-restricted CTL epitopes derived from SARS-CoV using HLA-A*0201 transgenic mice and recombinant adenovirus expressing predicted epitopes. These peptides were coupled to the surface of liposomes, and inoculated into mice. Two of the liposomal peptides were effective for peptide-specific CTL induction, and one of them was efficient for the clearance of vaccinia virus expressing epitopes of SARS-CoV, suggesting that the surface-linked liposomal peptide might offer an effective CTL-based vaccine against SARS.

1. Introduction

Severe acute respiratory syndrome (SARS) is a novel infectious disease that emerged in southern China in late 2002 and spread to several countries in early 2003. More than 8000 cases of SARS had been identified worldwide, and nearly 800 patients had died before the epidemic ended [1]. The etiologic agent of SARS has turned out to be a novel coronavirus termed SARS-associated coronavirus (SARS-CoV) [2–4], which is a plus-stranded RNA virus with an approximately 30-kb long genome encoding replicase gene products and the structural proteins containing spike (S), envelop (E), membrane (M), and nucleocapsid (N). Until now, the viral genome has been sequenced [5] and the viral receptor has been identified [6]. However, the pathogenesis of SARS remains poorly understood, and the apparent latency of SARS-CoV in animal reservoirs continuously provides us a serious threat of reemergence. Therefore, it is urgent to develop a new prophylactic and therapeutic strategy against SARS.

Among the four structural proteins of SARS-CoV, S protein interacts with the cellular receptor to mediate membrane fusion, allowing the virus to enter host cells [6]. Accordingly, S protein is a major target for neutralizing antibodies [7]. High titers of neutralizing antibodies to SARS-CoV were detected in sera of the recovered patients [8], and further, humoral immunity induced by a DNA vaccine contributed to the protection against SARS-CoV challenge in mice [7]. These data imply that neutralizing antibodies play a critical role in the clearance of SARS-CoV. On the other hand, a rapid loss of both $CD4^+$ and $CD8^+$ T cells was observed in patients suffering from severe SARS, and the cell counts gradually returned to normal ranges as the patients recovered [9]. Furthermore, certain HLA class I alleles have been reported to correlate with SARS susceptibility [10,11]. These data strongly suggest that, as with many other viral infections, virus-specific cytotoxic T lymphocytes (CTLs) should be important for viral elimination in SARS as well.

A synthetic peptide vaccine is a potential candidate for a CTL-based vaccine against pathogenic viruses on account of several advantages over conventional vaccines. First, synthetic peptides rarely cause undesirable responses including general toxicity, immunosuppression and autoimmunity. Second, it is possible to select short peptides in the absence of amino acid mutations. Third, synthetic peptides can easily be prepared as a pure immunogen in large quantities. However, a major disadvantage is the weak immunogenicity. Therefore, it is critical to search for adjuvant vehi-

* Corresponding author. Tel.: +81 49 276 1438; fax: +81 49 295 9107.
E-mail address: mmatsui@saitama-med.ac.jp (M. Matsui).

0264-410X/$ – see front matter © 2009 Elsevier Ltd. All rights reserved.
doi:10.1016/j.vaccine.2009.04.001

Table 1
Predicted CTL epitopes for SARS-CoV nucleocapsid protein.

Name	Position	Sequence	SYFPEITHI[a]	BIMAS[b]	BL_{50} (μM)[c]
N-113	113–122	YLGTGPEASL	98.3	26	25.7 ± 11.2
N-159	159–168	VLQLPQGTTL	309.1	29	235.3 ± 68.7
N-222	222–231	LLLLDRLNQL	69.6	24	52.6 ± 10.5
N-223	223–231	LLLDRLNQL	98.3	20	46.1 ± 4.9
N-227	227–235	RLNQLESKV	36.3	23	165.1 ± 36.6
N-317	317–325	GMSRIGMEV	1267.1	30	72.8 ± 37.7
N-331	331–340	WLTYHGAIKL	50.2	21	90.4 ± 39.2
N-352	352–360	ILLNKHIDA	31.2	19	140.5 ± 44.6

[a] Peptide binding scores to HLA-A2.1 were determined by the SYFPEITHI database [16] at http://www.syfpeithi.de/.
[b] Peptide binding scores to HLA-A2.1 were determined by the BIMAS database [17] at http://www-bimas.cit.nih.gov/molbio/hla_bind/.
[c] Data of peptide binding assays are shown as BL_{50}, indicating a concentration of each peptide that yields the half-maximal MFI of T2 cells pulsed with a control peptide, NS3-1585. Data are given as mean values ± SD of three independent experiments.

cles which are non-immunogenic themselves but which enhance the immunogenicity of peptides.

Liposomes have extensively been investigated as a delivery system for antigen [12]. In most cases, it has been prepared by antigen entrapment within the aqueous lumen of liposomes. In contrast, we have previously shown that ovalbulim (OVA) chemically conjugated on the surface of liposomes induced OVA-specific IgG production but not OVA-specific IgE production in mice [13], suggesting that the surface-linked liposomal antigen could offer a safe antigen delivery system without allergic side effects. Furthermore, we have demonstrated that an OVA-derived peptide, $OVA_{257-264}$ conjugated on the surface of liposomes made from unsaturated, but not saturated fatty acid, induced $OVA_{257-264}$-specific CTLs in mice more effectively than did liposomes containing $OVA_{257-264}$ inside [14,15]. In addition, it was shown that surface-linked liposomal peptides were able to provide tumor eradication [15] and protection against viral challenge [14] in mice. Taken together, these data suggest that liposomes would become an excellent adjuvant vehicle for a synthetic peptide vaccine when a peptide(s) is chemically coupled to the surface of liposomes.

In the current study, we explored the possibility that the surface-linked liposomal peptide might serve as an effective CTL-based vaccine against SARS. Firstly, we attempted to identify HLA-A*0201-restricted CTL epitopes derived from N protein of SARS-CoV (SARS-CoV-N) using computational algorithm, recombinant adenovirus and HLA-A*0201 transgenic mice. N protein was chosen for the analyses because this is more conserved than S protein. Peptides identified were then chemically conjugated on the surface of liposomes and evaluated for their abilities to induce SARS-CoV-N-specific CTLs and to clear virus using recombinant vaccinia virus expressing SARS-CoV-derived epitopes.

2. Materials and methods

2.1. Prediction of CTL epitopes

To define potential HLA-A*0201-binding peptides derived from SARS-CoV-N (Urbani strain) (GenBank accession number: AY278741), we used two computer-based programs, SYFPEITHI (http://www.syfpeithi.de/) [16] and BIMAS (http://www-bimas.cit.nih.gov/molbio/hla_bind/) [17]. As shown in Table 1, eight peptides (N-113, N-159, N-222, N-223, N-227, N-317, N-331, and N-352) with high scores were selected, and synthesized by Operon Biotechnologies (Tokyo, Japan). An I-A^b-restricted helper T cell peptide, hepatitis B virus (HBV) core 128 (amino acid sequence: TPPAYRPPNAPIL) [18] was also synthesized and used for immunization. Synthesized peptides were desalted, and analyzed by high performance liquid chromatography (HPLC).

2.2. Mice

Mice express a transgenic HLA-A*0201 monochain, designated as HHD, in which human beta-2 microglobulin (β2m) is covalently linked to a chimeric heavy chain composed of HLA-A*0201 (α1 and α2 domains) and H-$2D^b$ (α3, transmembrane, and cytoplasmic domains) [19,20]. Eight- to 12-week-old mice were used for all experiments. Mice were housed in appropriate animal care facilities at Saitama Medical University, Saitama, Japan, and handled according to international guidelines for experiments with animals.

2.3. Cell lines

A mouse lymphoma cell line transfected with the HHD gene, RMA-HHD (H-2^b) was previously described [19]. T2 [21] is a TAP-deficient, human lymphoblastoid cell line expressing natural HLA-A*0201. Human kidney cell lines, 293 and 293T cells were obtained from the American Type Culture Collection (Rockville, MD). African green monkey-derived kidney cell lines, CV-1 and BS-C-1, and a human osteosarcoma, thymidine kinase-defective cell line, C143 were kindly provided by Dr. T. Shioda (Osaka University, Japan). The T2 cell line was maintained in RPMI-1640 medium (Sigma–Aldrich, St. Louis, MO) supplemented with 10% fetal calf serum (FCS) (JRH Biosciences, Lenexa, KS) (R-10). The 293, 293T, CV-1, BS-C-1 and C143 cell lines were cultured in Dulbecco's modified Eagle's medium (DMEM) (Sigma–Aldrich) with 10% FCS (D-10). The RMA-HHD cell line was maintained in D-10 containing G418 (Sigma–Aldrich) at a final concentration of 500 μg/ml.

2.4. Peptide binding assay

Peptide binding assay was performed as described [22]. Briefly, T2 cells were incubated with a synthetic peptide at various concentrations overnight at 37 °C. Cells were stained with the anti-HLA-A*0201 monoclonal antibody (mAb), BB7.2 [23], followed by fluorescein isothiocyanate (FITC)-labeled goat anti-mouse IgG (Sigma–Aldrich). The mean fluorescence intensity (MFI) was measured by flow cytometry (FACScan, BD Biosciences, San Jose, CA). The concentration of each peptide that yields the half-maximal MFI of T2 cells pulsed with a control peptide derived from hepatitis C virus (HCV), NS3-1585 [22] was calculated as the half-maximal binding level (BL_{50}). Experiments were performed three times, and data are given as mean values ± SD.

2.5. Construction of a multiepitope minigene

A multiepitope minigene that encodes the eight predicted epitopes with 5–11 natural flanking amino acid residues at both of the N and C termini (Fig. 1) (SARS-N8E) was constructed using

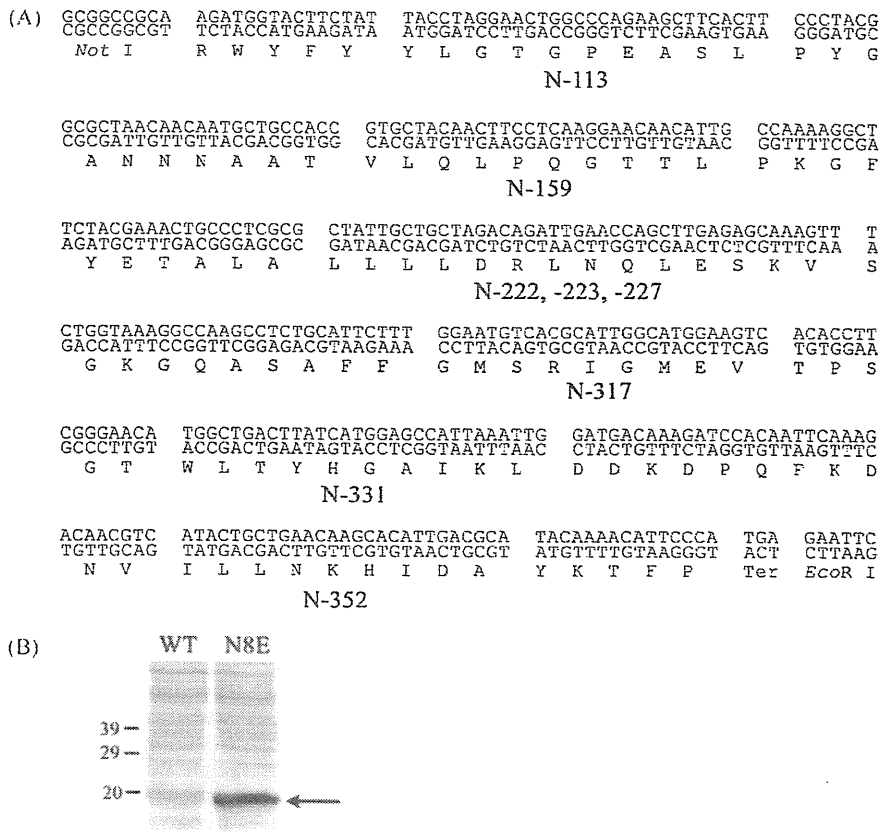

Fig. 1. (A) Nucleotide and amino acid sequences of eight predicted epitopes (N-113, N-159, N-222, N-223, N-227, N-317, N-331 and N-352) with flanking amino acid residues encoded in a minigene, termed SARS-N8E. (B) Expression of the SARS-N8E fusion protein. 293 T cells were infected with either Ad-WT (WT) or Ad-SARS-N8E (N8E). After 2 days' incubation, cells were lysed and separated on by SDS-12% polyacrylamide gel electrophoresis and subjected to Western blotting analysis with the anti-FLAG antibody. The positions of protein molecular mass markers (in kDa) are shown in the figure, and an arrow indicates the band of the SARS-N8E fusion protein.

overlapping long oligonucleotides in PCR-based synthesis [24]. In brief, five long oligos, averaging about 90 nucleotides in length with 20–25 nucleotide overlaps, were synthesized and HPLC-purified by Operon Biotechnologies. The minigene was then assembled by extending the five overlapping oligos. After confirming the nucleotide sequence by DNA sequencing, the multiepitope minigene, SARS-N8E was cloned into the NotI and EcoRI sites of p3xFLAG-CMV-10 expression vector (Sigma–Aldrich) (p3xFLAG-SARS-N8E). This vector encodes the three adjacent FLAG-tag epitopes (amino acid sequence: DYKDHDGDYKDHDIDYKDDDDK) upstream of the multiple cloning region, and hence, expresses an N-terminal 3xFLAG fusion protein under the control of the CMV promoter in mammalian cells.

2.6. Generation of recombinant adenovirus and vaccinia virus expressing multiple CTL epitopes

Recombinant adenovirus expressing the eight predicted epitopes (Ad-SARS-N8E) was generated using the Adenovirus Expression Vector Kit (Takara Bio Inc., Shiga, Japan). Briefly, the SARS-N8E minigene linked to the 3xFLAG-tag sequence was isolated by PCR amplification from p3xFLAG-SARS-N8E, and inserted into the cloning site of the cosmid vector, pAxCAwtit containing the entire adenovirus genome except for the E1 and E3 genes. This recombinant cosmid was co-transfected with DNA-TPC containing the adenovirus terminal protein into 293 cells by Lipofectamine 2000 (Invitrogen, Carlsbad, CA). Since 293 cells express E1A and E1B, replication-defective adenovirus can be produced. After cloning, virus was amplified in 293 cells and titered by standard plaque assays on 293 cells. Wild-type adenovirus (Ad-WT) was used as a negative control.

Recombinant vaccinia virus (WR strain) expressing the eight predicted epitopes (VV-SARS-N8E) was generated as described before [25]. In brief, the SARS-N8E minigene with the 3xFLAG-tag sequence was inserted into the transfer vector, pNZ(
N8E was then generated by homologous recombi
wild-type vaccinia virus (VV-WT) and the transfer
by three cycles of plaque cloning with C143 cells in
bromodeoxyuridine, and propagated in CV-1 cells. Viral titers were measured by standard plaque assays on BS-C-1 cells.

To detect expression of the SARS-N8E fusion protein, Western blotting was performed as described previously [25]. In brief, 293T cells were infected with Ad-SARS-N8E at a multiplicity of infection (MOI) of 30 or VV-SARS-N8E at an MOI of 3 for 1.5 h. After 2 days' incubation, cells were lysed and the solubilized proteins were separated by electrophoresis on a 12% SDS-PAGE under reducing condition, and blotted onto a nitrocellulose membrane. The blot was stained with 5 μg/ml of the anti-FLAG M2 mAb (Sigma–Aldrich), followed by secondary staining with peroxidase conjugated anti-mouse IgG Ab. The protein bands were developed by the BCIP/NBT Phosphatase Substrate System (KPL Inc., Gaithersburg, MD).

2.7. Surface-linked liposomal peptides

Oleoyl liposomes are composed of dioleoyl phosphatidyl choline, dioleoyl phosphatidyl ethanolamine, dioleoyl phosphatidyl glycerol acid, and cholesterol in a 4:3:2:7 molar ratio [26].

Each of CTL peptides and a helper peptide was then coupled to the surface of liposomes at a same molar concentration via disuccinimidyl suberate (DSS) as described previously [15]. Empty liposomes were used as a negative control.

2.8. Immunization

For identification of CTL epitopes, mice were immunized intraperitoneally (i.p.) with 5×10^8 plaque-forming units (PFU) of either Ad-WT or Ad-SARS-N8E. For the immunization with liposomal peptides, mice were subcutaneously (s.c.) immunized with each surface-linked liposomal CTL peptide (25 μg/mouse) mixed with a liposomal helper peptide (25 μg/mouse) and CpG-ODN (5′-TCCATGACGTTCTGATGTT-3′, Hokkaido System Science, Sapporo, Japan) (5 μg/mouse) in 100 μl PBS in the footpad.

2.9. Intracellular IFN-γ staining

Intracellular cytokine staining (ICS) was performed as described previously [27]. Briefly, after 1 week following immunization, spleen cells of immunized mice were incubated with brefeldin A (GolgiPlug, BD Biosciences) for 5 h at 37 °C in the presence or absence of a relevant peptide at a final concentration of 10 μM. After incubation with the rat anti-mouse CD16/CD32 mAb (Fc Block, BD Biosciences), cells were stained with FITC-conjugated rat anti-mouse CD8α mAb (BD Biosciences) for 30 min at 4 °C. Cells were then fixed, permeabilized, and stained with phycoerythrin (PE)-conjugated rat anti-mouse IFN-γ mAb (BD Biosciences). After washing the cells, flow cytometric analyses were performed.

2.10. ^{51}Cr-release assay

^{51}Cr-release assays were carried out as described before [19]. In brief, after 2 weeks following immunization, spleen cells of immunized mice were cultured for 1 week with irradiated (30 Gy), syngeneic naive spleen cells pre-pulsed with 10 μM of a relevant peptide, and employed as effector cells in standard ^{51}Cr-release assays. RMA-HHD cells were pulsed with or without 10 μM of each peptide for 1 h, labeled with 100 μCi of $Na_2{}^{51}CrO_4$, and used for target cells. After a 4-h incubation, supernatant of each well was harvested and the radioactivity was counted. Results were calculated as the mean of a triplicate assay. Percent specific lysis was calculated according to the formula: % specific lysis = $[(cpm_{sample} - cpm_{spontaneous})/(cpm_{maximum} - cpm_{spontaneous})] \times 100$. Spontaneous release represents the radioactivity released by target cells in the absence of effectors, and maximum release represents the radioactivity released by target cells lysed with 5% Triton X-100.

2.11. In vivo CTL assay

In vivo CTL assay was carried out as reported before [28]. Briefly, spleen cells from naive HHD mice were equally split into two populations. One population was pulsed with a peptide at a final concentration of 10 μM for 1 h at 37 °C, and then labeled with a high concentration (2.5 μM) of carboxyfluorescein diacetate succinimidyl ester (CFSE) (Molecular Probes, Eugene, OR) for 10 min at 37 °C ($CFSE^{high}$). The other was unpulsed and labeled with a lower concentration (0.25 μM) of CFSE ($CFSE^{low}$). An equal number (1×10^7) of cells from each population was mixed and transferred intravenously (i.v.) into mice that had been immunized 1 week earlier. Twelve hours later, spleen cells were prepared and analyzed by flow cytometry. To calculate specific lysis, the following formula was used: % specific lysis = [1 − {(number of $CFSE^{low}$ cells in normal mice)/(number of $CFSE^{high}$ cells in normal mice)}/{(number of $CFSE^{low}$ cells in immunized mice)/(number of $CFSE^{high}$ cells in immunized mice)}] × 100.

2.12. Viral challenge

Viral challenge experiments were performed as described before [29]. Two weeks after immunization, mice were challenged i.p. with 1×10^6 PFU of either VV-SARS-N8E or VV-WT. Five days later, mice were sacrificed, and two ovaries of each mouse were homogenized, and resuspended in 0.5 ml of PBS containing 1% FCS and 1 mM $MgCl_2$. Virus was released from the cells by three freeze–thaw cycles followed by sonication. Viral titers were measured by plating serial 10-fold dilutions on BS-C-1 indicator cells in 6-well plates. All titrations were performed in duplicates, and the average PFU per mouse was calculated.

2.13. Statistical analyses

Statistical analyses were performed with Student's *t*-test. A value of $P < 0.05$ was considered statistically significant.

3. Results

3.1. Prediction of CTL epitopes derived from SARS-CoV-N

The amino acid sequence of SARS-CoV-N was searched for potential HLA-A*0201-restricted CTL epitopes by two computer-based programs, SYFPEITHI [16] and BIMAS [17]. According to the scores calculated, eight nonameric and decameric peptides were selected and synthesized (Table 1). To evaluate the binding affinity of these peptides to HLA-A*0201 molecules, the peptide binding assay [22] was performed (Table 1). Five (N-113, N-222, N-223, N-317, and N-331) out of the eight peptides were high binders displaying BL_{50} values less than 100 μM, and two (N-227 and N-352) of them were medium binders displaying BL_{50} values ranging from 100 to 200 μM. These data suggest that prediction of CTL epitopes should be mostly successful. In contrast, one peptide, N-159 showed low affinity binding.

3.2. Induction of SARS-CoV-N-specific CTLs in HHD mice infected with adenovirus

To investigate whether CTLs specific for the predicted peptides were elicited, HHD mice were immunized i.p. once with either Ad-SARS-N8E or Ad-WT. One week after immunization, spleen cells were prepared and stimulated with each of the eight predicted peptides derived from SARS-CoV-N for 5 h. Cells were then stained for their surface expression of CD8 and antigen-induced intracellular expression of IFN-γ. As shown in Fig. 2, considerable numbers of IFN-γ-producing $CD8^+$ T cells were induced by stimulation with peptides including N-222, N-223, N-227 and N-317 in Ad-SARS-N8E-infected mice but not in Ad-WT-injected mice, indicating that CTLs specific for these four peptides were induced in mice by immunization with Ad-SARS-N8E. In contrast, none of the remaining peptides significantly elicited IFN-γ-secreting $CD8^+$ T cells (Fig. 2).

We next examined peptide-specific killing activities in spleen cells of mice that had been immunized with Ad-SARS-N8E. Two weeks after immunization, spleen cells of the mice were harvested and stimulated *in vitro* with each of the peptides. One week later, ^{51}Cr-release assays were performed at various effector:target (E:T) ratios. In agreement with the data of ICS (Fig. 2), the four peptides, N-222 (Fig. 3C), N-223 (Fig. 3D), N-227 (Fig. 3E) and N-317 (Fig. 3F) elicited strong peptide-specific CTL responses in Ad-SARS-N8E-infected mice but not in Ad-WT-infected mice. On the other

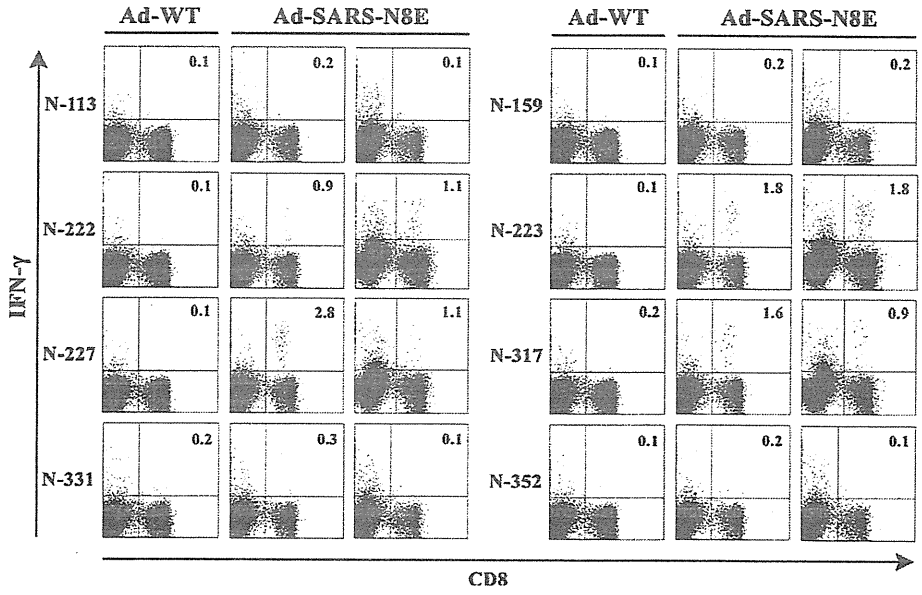

Fig. 2. Intracellular IFN-γ staining of CD8⁺ T cells specific for SARS-CoV-N-derived peptides in spleen cells of mice immunized with either Ad-SARS-N8E or Ad-WT. HHD mice were immunized i.p. once with either Ad-SARS-N8E or Ad-WT. One week later, spleen cells were prepared and stimulated with each of the eight predicted peptides (N-113, N-159, N-222, N-223, N-227, N-317, N-331, and N-352) for 5 h. Cells were then stained for their surface expression of CD8 (*x*-axis) and their intracellular expression of IFN-γ (*y*-axis). The numbers shown indicate the percentages of intracellular IFN-γ⁺ cells within CD8⁺ T cell. The data shown are representative of three independent experiments.

hand, the remaining peptides, N-113 (Fig. 3A), N-159 (Fig. 3B), N-331 (Fig. 3G), and N-352 (Fig. 3H) failed to induce CTL activities in either Ad-SARS-N8E-injected mice or Ad-WT-injected mice. To further address peptide-specific killing activities in mice, *in vivo* CTL assays were carried out (Fig. 4). After immunization with either Ad-WT or Ad-SARS-N8E, HHD mice received i.v. injection of peptide-pulsed $CFSE^{high}$ targets and unpulsed $CFSE^{low}$ targets. Twelve hours later, spleen cells were prepared and peptide-specific lysis was assessed by flow cytometry. As was expected, N-222-, N-223-, N-227- and N-317-specific CTL killing activities were significantly detected in mice immunized with Ad-SARS-N8E, but not in Ad-WT-injected mice (Fig. 4). Especially, the activity of N-223-specific killing was greatest (Fig. 4), suggesting that N-223 might be an immunodominant epitope. Any of the remaining peptides, N-113, N-159, N-331 and N-352 could not induce peptide-specific killing activities in *in vivo* CTL assays (data not shown).

3.3. *Induction of SARS-CoV-N-specific CTLs by immunization with surface-linked liposomal peptides*

We next investigated whether surface-linked liposomal peptides could induce peptide-specific CTLs in mice. Since four peptides including N-222, N-223, N-227 and N-317 were expected to be HLA-A*0201-restricted CTL epitopes (Figs. 2–4), these peptides were chemically conjugated on the surface of liposomes. Surface-linked liposomal peptides, Lip-N222, Lip-N223, Lip-N227 and Lip-N317 were then evaluated for their capabilities of CTL induction in HHD mice. One week after immunization with each of the liposomal peptides, spleen cells were prepared, stimulated with a relevant peptide, and stained for their expression of surface CD8 and intracellular IFN-γ. As shown in Fig. 5, significant numbers of IFN-γ-producing CD8⁺ T cells were elicited in mice that had been immunized once with either Lip-N223 or Lip-N227 in the footpad. In the case of Lip-N317, however, one injection with Lip-N317 did not result in the induction of IFN-γ-producing CD8⁺ T cells (Fig. 5), and after three injections, a significant expansion of IFN-γ-producing CD8⁺ T cells in response to N-317 was finally observed (Fig. 5), indicating that Lip-N317 might be less immunogenic than Lip-N223 and Lip-N227. On the other hand, Lip-N222 failed to elicit N-222-specific IFN-γ-producing CD8⁺ T cells in mice (Fig. 5) even after multiple injections. Since N-222 is a 10-mer peptide composed of an N-223 peptide with one additional leucine at the N-terminus (Table 1), there was a possibility of cross reaction between N-222 and N-223. As shown in Fig. 6, both N-222 and N-223 peptides obviously stimulated IFN-γ-producing CD8⁺ T cells in mice immunized with Lip-N223, demonstrating that N-223-specific CTLs primed by Lip-N223 was activated by stimulation with N-222 as well as N-223. In contrast, either N-222 or N-223 could not induce IFN-γ-secreting CD8⁺ T cells in mice primed with Lip-N222.

3.4. *Administration of Lip-N223 provided protective immunity in mice against virus challenge*

Because Lip-N223 and Lip-N227 effectively primed IFN-γ-producing CD8⁺ T cells in mice (Fig. 5), we next evaluated whether immunization with either Lip-N223 or Lip-N227 would induce CD8⁺ CTLs to kill peptide-pulsed target cells *in vivo*. One week after immunization of mice, both peptide-pulsed $CFSE^{high}$ target cells and unpulsed $CFSE^{low}$ target cells were delivered into the mice via i.v. injection. As shown in Fig. 7, the peptide-specific killing activity in Lip-N223-immunized mice was greater than that in Lip-N227-immunized mice, indicating that Lip-N223 was more immunogenic than Lip-N227. Therefore, we next tested whether mice immunized with Lip-N223 were able to clear virus challenged. HHD mice were immunized twice with Lip-N223 at a 2-week interval. Two weeks after the last immunization, the mice were challenged with 1×10^6 PFU of VV-SARS-N8E or VV-WT. After 5 days following the challenge, viral titers were measured in two ovaries of each mouse. As shown in Fig. 8, titers of vaccinia virus in mice challenged with VV-SARS-N8E were 3 logs lower than those in mice challenged with VV-WT. Mice immunized with empty liposomes retained high viral titers after challenge with either VV-SARS-N8E (Fig. 8) or VV-WT (data not shown). Thus, these data indicate that immunization with Lip-N223 is effective in the protection against virus.

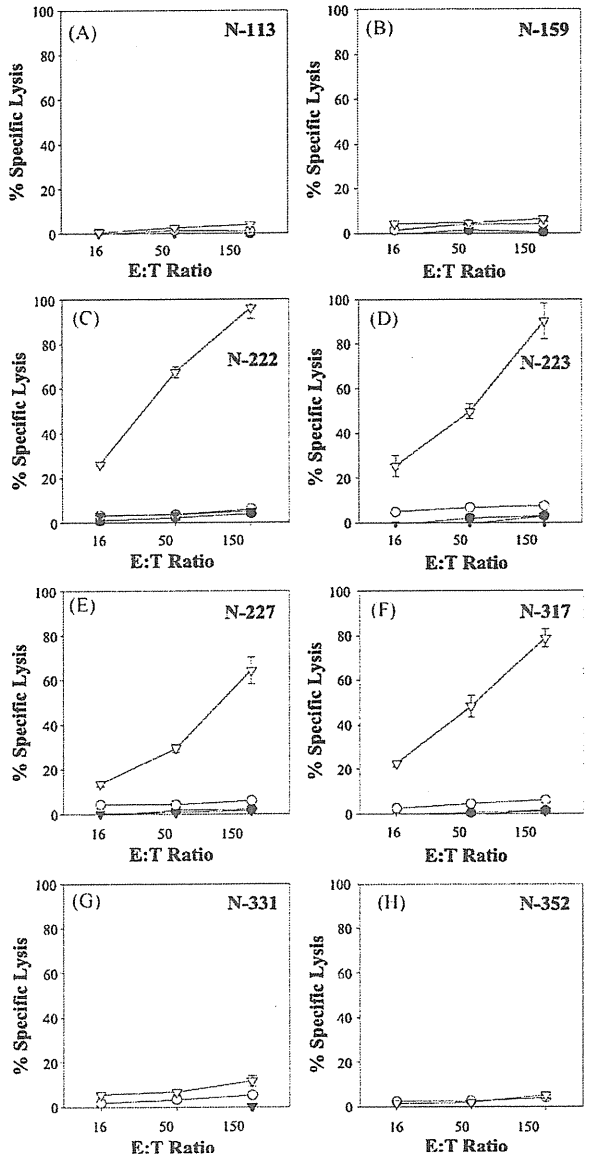

Fig. 3. CTL activities specific for eight predicted epitopes derived from SARS-CoV-N in mice immunized with Ad-SARS-N8E. HHD mice were immunized i.p. with either Ad-SARS-N8E (reverse triangles) or Ad-WT (circles). Two weeks after immunization, spleen cells were prepared and stimulated *in vitro* with each of the eight predicted epitopes (N-113, N-159, N-222, N-223, N-227, N-317, N-331, and N-352) derived from SARS-CoV N protein. After 1 week, ^{51}Cr-release assays were performed at various E:T ratios with RMA-HHD cells pulsed with (open symbols) or without (solid symbols) a relevant peptide as target. Data are shown as the means ± SD of triplicate wells. The experiment was repeated twice with similar results. At least three mice per group were used in each experiment.

4. Discussion

Since S protein is responsible for binding to specific cellular receptors [6], this is a major target for neutralizing antibodies [7]. Moreover, vigorous S-specific CTL responses were generated in SARS-CoV-infected patients [30,31], indicating that S protein is an antigen for CTL as well. In fact, four CTL epitopes derived from S protein have been identified [31–33]. However, since N protein is more conserved and synthesized earlier than S protein, N protein seems preferable to S protein as an antigenic target for T-cell immunity. Therefore, we focused on SARS-CoV N protein for the development of a CTL-based vaccine in the current study.

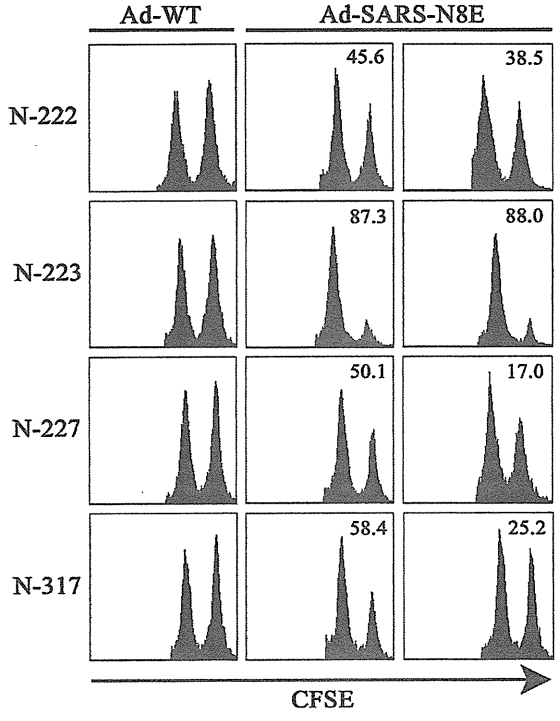

Fig. 4. *In vivo* killing of peptide-pulsed target cells in HHD mice immunized with Ad-SARS-N8E. HHD mice were immunized with either Ad-WT or Ad-SARS-N8E. One week later, an equal number of each peptide (N-222, N-223, N-227, or N-317)-pulsed $CFSE^{high}$ targets and unpulsed $CFSE^{low}$ targets were transferred into the immunized mice by i.v. injection. After 12 h, CFSE-labeled cells were recovered from spleens of recipient mice and analyzed by flow cytometry. The experiment was repeated three times with similar results. The numbers show the percentages of specific lysis.

High-performing computational algorithms have extensively been used for the identification of CTL epitopes [18,31–34]. Chentoufi et al. [34] supported their predictive computational algorithms by multiple immunological screenings. Thus, it is important to use multiple screenings for successful identification of functional CTL epitopes. We also performed multiple immunological screens, including cell surface stabilization of HLA-A*0201 molecules on T2 cells, detection of antigen-driven IFN-γ-producing $CD8^+$ T cells, and functional *in vivo* and *in vitro* CTL assays. Our strategy for the identification of CTL epitopes has several advantages. First, the use of recombinant adenovirus and vaccinia virus allowed us to circumvent the necessity for handling live SARS-CoV. Both of the recombinant viruses, Ad-SARS-N8E and VV-SARS-N8E, carry the multiepitope minigene that encodes eight predicted epitopes with several natural flanking amino acid residues at both of the ends, thereby offering natural antigen processing in the infected cells. The basic idea comes from the observation that flanking sequences proximal to CTL epitopes modulate proteasomal processing of the epitopes [35,36]. Furthermore, we can carry out *in vitro* and *in vivo* experiments using these viruses in BSL-2 facilities. Replication-defective recombinant adenovirus effectively induces CTLs specific for a protein encoded by a gene inserted into the viral genome [29,37,38]. Recombinant vaccinia virus can be employed as a virus challenged in the protection experiment [29,39]. Second, we used highly reactive HLA-A*0201 transgenic mice, termed HHD mice [20]. Because the innate $H\text{-}2D^b$ and mouse β2m genes have been disrupted by homologous recombination in HHD mice, the only MHC class I molecule on the cell surface, HLA-A*0201, is efficiently utilized by HLA- A*0201-restricted CTLs. We used lymphocytes of HHD mice infected with Ad-SARS-N8E as a replacement for PBL of SARS patients. As a consequence, we identified three HLA-

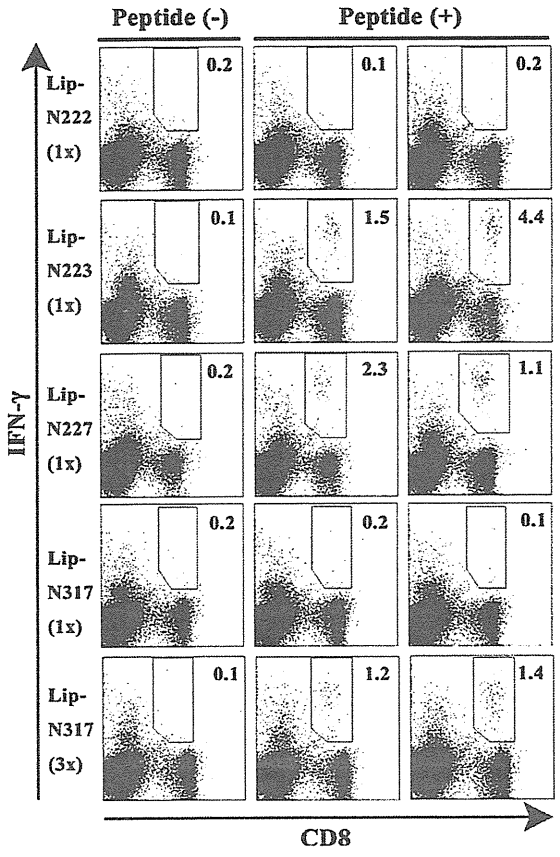

Fig. 5. Intracellular IFN-γ staining of $CD8^+$ T cells specific for SARS-CoV-N-derived peptides in spleen cells of mice immunized with surface-linked liposomal peptides. HHD mice received one injection (1×) of either Lip-N222, Lip-N223, Lip-N227 or Lip-N317, or three injections (3×) of Lip-N317 together with a liposomal helper peptide and CpG. After 1 week, spleen cells were prepared and stimulated with a relevant peptide (N-222, N-223, N-227 or N-317) for 5 h. Cells were then stained for their surface expression of CD8 (*x*-axis) and their intracellular expression of IFN-γ (*y*-axis). The numbers shown indicate the percentages of intracellular IFN-γ^+ cells within $CD8^+$ T cell. The data shown are representative of three independent experiments.

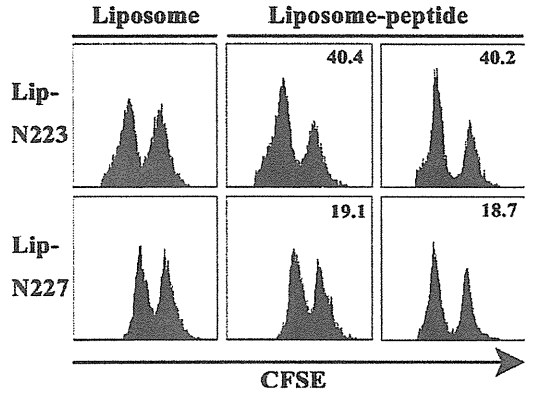

Fig. 7. *In vivo* killing activities specific for N-223 and N-227 in HHD mice immunized with surface-linked liposomal peptides. HHD mice were immunized once with either Lip-N223 or Lip-N227 together with a liposomal helper peptide and CpG in the footpad. One week later, an equal number of a relevant peptide (N-223 or N-227)-pulsed $CFSE^{high}$ targets and unpulsed $CFSE^{low}$ targets were transferred into the immunized mice by i.v. injection. After 12 h, CFSE-labeled cells were recovered from spleens of recipient mice and analyzed by flow cytometry. The numbers show the percentages of specific lysis. The experiment was repeated twice.

A*0201-restricted CTL epitopes, N-223, N-227, and N-317, derived from SARS-CoV-N, which were identical to those reported by Tsao et al. [40]. This indicates that our approach has proved to be practical in the epitope identification for viruses. However, it has to be taken account that there may be differences between the immunogenic variations observed in HLA class I transgenic mice and that in humans primarily because the antigen processing, presentation and ultimately, immunodominance may differ between them. Further, it will be necessary to use SARS-CoV for viral challenge experiments at the final stage.

N-222 peptide is unlikely to be an epitope because N-222-specific CTLs could not be induced by immunization with Lip-N222 (Fig. 5). However, N-223-specific CTLs primed by Lip-N223 were activated by stimulation with N-222 as well as N-223 (Fig. 6). Accordingly, when interpreting the data concerning N-222 in Figs. 2–4, we could propose an explanation that immunization of mice with Ad-SARS-N8E did not induce N-222-specific CTLs but

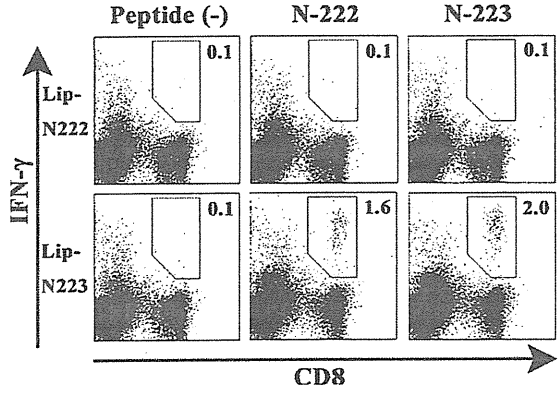

Fig. 6. Cross reactivity between N-222 and N-223 peptides. HHD mice were immunized with either Lip-N222 or Lip-N-223 together with a liposomal helper peptide and CpG in the footpad. One week later, spleen cells were prepared and stimulated *in vitro* with or without either N-222 or N-223 for 5 h. Cells were then stained for their surface expression of CD8 (*x*-axis) and their intracellular expression of IFN-γ (*y*-axis). The numbers shown indicate the percentages of intracellular IFN-γ^+ cells within $CD8^+$ T cell. The experiment was repeated twice with similar results.

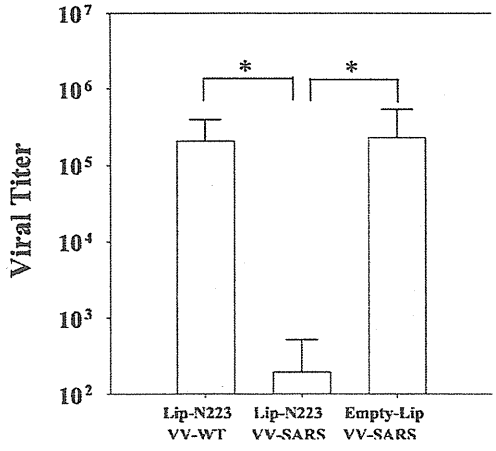

Fig. 8. Resistance to infection with vaccinia virus expressing N-223 in mice immunized with Lip-N223. HHD mice were immunized twice with either Lip-N223 or empty liposomes (Empty-Lip) along with a liposomal helper peptide and CpG at 2-week intervals. Two weeks later, mice were challenged i.p. with 1×10^6 PFU of either VV-SARS-N8E (VV-SARS) or VV-WT. Mice were then sacrificed 5 days after challenge, and viral titers in the ovaries were measured. All titrations were performed in duplicates, and the average PFU per mouse is shown in the figure. Three mice were used in each group, and data are shown as the mean ± SD of three mice. *$P < 0.01$.

did N-223-specific CTLs, which recognized N-222 as well as N-223 (Figs. 2–4).

In the current study, we have shown that surface-linked liposomal peptides such as Lip-N223 and Lip-N227 were very effective for the induction of peptide-specific CTLs in mice as well as recombinant adenovirus, Ad-SARS-N8E (Figs. 2 and 5). Of note, the most immunogenic liposomal peptide, Lip-N223 efficiently induced protection against viral challenge with vaccinia virus expressing N-223 (Fig. 8). These data strongly suggest that the surface-linked liposomal peptide may offer an effective and safe CTL-based vaccine against SARS. However, *in vivo* CTL activity induced by Lip-N223 immunization was half of that induced by Ad-SARS-N8E (Figs. 4 and 7) although the level of IFN-γ-producing $CD8^+$ T cells was similar between the Ad-SARS-N8E and Lip-N223 immunization (Figs. 2 and 5). These data might suggest that liposomes disturb the CTL killing activity in some degree. Furthermore, a number of IFN-γ-producing $CD8^+$ T cells specific for N-317 were elicited in mice that had received one injection of Ad-SARS-N8E (Fig. 2). In contrast, three injections of Lip-N317 were required for the significant induction of N-317-specific IFN-γ-producing $CD8^+$ CTLs in mice (Fig. 5). These data might suggest that an exogenous peptide conjugated on the surface of liposomes may be processed and presented to peptide-specific CTLs in a different way from a naturally processed, endogenous peptide derived from adenovirus.

Our surface-linked liposomal peptide might be similar to the lipopeptide, a form of palmitoyl-lipidated peptide that is currently under intense investigation as human vaccines for many infectious pathogens and cancers [41–43]. Although both effectively induce peptide-specific CTLs, there are several differences between them. Fist of all, self-adjuvanting lipopeptides stimulate peptide-specific CTLs via Toll-like receptor (TLR)-2 without any particular adjuvants [42,43]. In contrast, induction of CTLs by surface-linked liposomal peptides requires external TLR ligands such as CpG [14]. However, it is well known that CpG causes toxicity in humans [44]. Hence, it is essential to find out a safe adjuvant for clinical use of liposomal peptides. Second, lipopeptides administered intranasally, sublingually or intravaginally are able to induce mucosal and systemic immune responses [43]. This application offers the advantage of needle-free delivery. It is, however, still under investigation whether surface-linked liposomal peptides intranasally stimulate peptide-specific CTLs.

In summary, we first tried to identify HLA-A*0201-restricted CTL epitopes derived N protein of SARS-CoV using computational algorithm, recombinant adenovirus and HLA-A*0201 transgenic mice. Four peptides that were expected to be epitopes were then chemically conjugated on the surface of liposomes. It was shown that two of the liposomal peptides were effective for peptide-specific CTL induction, and the most immunogenic liposomal peptide efficiently induced protection against viral challenge with vaccinia virus expressing this peptide. These data suggest that the surface-linked liposomal peptide may be useful for CTL-based immunotherapy against SARS.

Acknowledgments

This work was supported by a grant from The Ministry of Health, Labor and Welfare of Japan. The authors are grateful to Dr. F.A. Lemonnier (Pasteur Institute, Paris, France) for providing HHD mice and the RMA-HHD cell line, and to Dr. T. Shioda for providing CV-1, BS-C-1, C143 cell lines, and vaccinia virus (WR strain).

References

[1] Groneberg DA, Zhang L, Welte T, Zabel P, Chung KF. Severe acute respiratory syndrome: global initiatives for disease diagnosis. Q J Med 2003;96(11):845–52.
[2] Drosten C, Gunther S, Preiser W, van der Werf S, Brodt HR, Becker S, et al. Identification of a novel coronavirus in patients with severe acute respiratory syndrome. N Engl J Med 2003;348(20):1967–76.
[3] Ksiazek TG, Erdman D, Goldsmith CS, Zaki SR, Peret T, Emery S, et al. A novel coronavirus associated with severe acute respiratory syndrome. N Engl J Med 2003;348(20):1953–66.
[4] Peiris JSM, Lai ST, Poon LLM, Guan Y, Yam LYC, Lim W, et al. Coronavirus as a possible cause of severe acute respiratory syndrome. Lancet 2003;361(9371):1319–25.
[5] Marra MA, Jones SJM, Astell CR, Holt RA, Brooks-Wilson A, Butterfield YSN, et al. The genome sequence of the SARS-associated coronavirus. Science 2003;300(5624):1399–404.
[6] Li W, Moore MJ, Vasilieva N, Sui J, Wong SK, Berne MA, et al. Angiotensin-converting enzyme 2 is a functional receptor for the SARS coronavirus. Nature 2003;426(6965):450–4.
[7] Yang Z, Kong W, Huang Y, Roberts A, Murphy BR, Subbarao K, et al. A DNA vaccine induces SARS coronavirus neutralization and protective immunity in mice. Nature 2004;428(6982):561–4.
[8] Li G, Chen X, Xu A. Profile of specific antibodies to the SARS-associated coronavirus. N Engl J Med 2003;349(5):508–9.
[9] Tang X, Yin C, Zhang F, Fu Y, Chen W, Chen Y, et al. Measurement of subgroups of peripheral blood T lymphocytes in patients with severe acute respiratory syndrome and its clinical significance. Chin Med J 2003;116(6):827–30.
[10] Lin M, Tseng HK, Trejaut JA, Lee HL, Loo JH, Chu CC, et al. Association of HLA class I with severe acute respiratory syndrome coronavirus infection. BMC Med Genet 2003;4:9–15.
[11] Ng MHL, Lau KM, Li L, Cheng SH, Chan WY, Hui PK, et al. Association of human-leukocyte-antigen class I (B*0703) and class II (DRB1*0301) genotypes with susceptibility and resistance to the development of severe acute respiratory syndrome. J Infect Dis 2004;190(3):515–8.
[12] Alving CR, Koulchin V, Glenn GM, Rao M. Liposomes as carriers of peptide antigens: induction of antibodies and cytotoxic T lymphocytes to conjugated and unconjugated peptides. Immunol Rev 1995;145:5–31.
[13] Taneichi M, Naito S, Kato H, Tanaka Y, Mori M, Nakano Y, et al. T cell-independent regulation of IgE antibody production induced by surface-linked liposomal antigen. J Immunol 2002;169(8):4246–52.
[14] Nagata T, Toyota T, Ishigaki H, Ichihashi T, Kajino K, Kashima Y, et al. Peptides coupled to the surface of a kind of liposome protect infection of influenza viruses. Vaccine 2007;25(26):4914–21.
[15] Taneichi M, Ishida H, Kajino K, Ogasawara K, Tanaka Y, Kasai M, et al. Antigen chemically coupled to the surface of liposomes are cross-presented to $CD8^+$ T cells and induce potent antitumor immunity. J Immunol 2006;177(4):2324–30.
[16] Rammensee HG, Bachmann J, Emmerich NPN, Bachor OA, Stevanovic S. SYFPEITHI: database for MHC ligands and peptide motifs. Immunogenetics 1999;50(3–4):213–9.
[17] Parker KC, Bednarek MA, Coligan JE. Scheme for ranking potential HLA-A2 binding peptides based on independent binding of individual peptide side-chains. J Immunol 1994;152(1):163–75.
[18] Botten J, Alexander J, Pasquetto V, Sidney J, Barrowman P, Ting J, et al. Identification of protective Lassa virus epitopes that are restricted by HLA-A2. J Virol 2006;80(17):8351–61.
[19] Matsui M, Moriya O, Belladonna ML, Kamiya S, Lemonnier FA, Yoshimoto T, et al. Adjuvant activities of novel cytokines, interleukine (IL)-23 and IL-27 for induction of hepatitis C virus-specific cytotoxic T lymphocytes in HLA-A*0201 transgenic mice. J Virol 2004;78(17):9093–104.
[20] Pascolo S, Bervas N, Ure JM, Smith AG, Lemonnier FA, Perarnau B. HLA-A2 1-restricted education and cytolytic activity of $CD8^+$ T lymphocytes from β2 microglobulin (β2m) HLA-A2.1 monochain transgenic $H\text{-}2D^b$ β2m double knockout mice. J Exp Med 1997;185(12):2043–51.
[21] Salter RD, Howell DN, Cresswell P. Genes regulating HLA class I antigen expression in T–B lymphoblast hybrids. Immunogenetics 1985;21(3):235–46.
[22] Ohno S, Moriya O, Yoshimoto T, Hayashi H, Akatsuka T, Matsui M. Immunogenic variation between multiple HLA-A*0201-restricted, hepatitis C virus-derived epitopes for cytotoxic T lymphocytes. Viral Immunol 2006;19(3):458–67.
[23] Parham P, Brodsky FM. Partial purification and some properties of BB7.2: a cytotoxic monoclonal antibody with specificity for HLA-A2 and a variant of HLA-A28. Hum Immunol 1981;3(4):277–99.
[24] Ishioka GY, Fikes J, Hermanson G, Livingston B, Crimi C, Qin M, et al. Utilization of MHC class I transgenic mice for development of minigene DNA vaccines encoding multiple HLA-restricted CTL epitopes. J Immunol 1999;162(7):3915–25.
[25] Kohyama S, Ohno S, Isoda A, Moriya O, Belladonna ML, Hayashi H, et al. IL-23 enhances host defense against vaccinia virus infection via a mechanism partly involving IL-17. J Immunol 2007;179(6):3917–25.
[26] Nakano Y, Mori M, Nishinohara S, Takita Y, Naito S, Kato H, et al. Surface-linked liposomal antigen induces IgE-selective unresponsiveness regardless of the lipid components of liposomes. Bioconjug Chem 2001;12(3):391–5.
[27] Matsui M, Moriya O, Yoshimoto T, Akatsuka T. T-bet is required for protection against vaccinia virus infection. J Virol 2005;79(20):12798–806.
[28] Suvas S, Kumaraguru U, Pack CD, Lee S, Rouse BT. $CD4^+CD25^+$ T cells regulate virus-specific primary and memory $CD8^+$ T cell responses. J Exp Med 2003;198(6):889–901.
[29] Matsui M, Moriya O, Akatsuka T. Enhanced induction of hepatitis C virus-specific cytotoxic T lymphocytes and protective efficacy in mice by DNA vaccination followed by adenovirus boosting in combination with the interleukin-12 expression plasmid. Vaccine 2003;21(15):1629–39.

[30] Chen H, Hou J, Jiang X, Ma S, Meng M, Wang B, et al. Response of memory CD8+ T cells to severe acute respiratory syndrome (SARS) coronavirus in recovered SARS patients and healthy individuals. J Immunol 2005;175(1):591–8.
[31] Wang YD, Sin WYF, Xu GB, Yang HH, Wong T, Pang XW, et al. T-cell epitopes in severe acute respiratory syndrome (SARS) coronavirus spike protein elicit a specific T-cell immune response in patients who recover from SARS. J Virol 2004;78(11):5612–8.
[32] Wang B, Chen H, Jiang X, Zhang M, Wan T, Li N, et al. Identification of an HLA-A*0201-restricted CD8+ T-cell epitope SSp-1 of SARS-CoV spike protein. Blood 2004;104(1):200–6.
[33] Zhou M, Xu D, Li X, Li H, Shan M, Tang J, et al. Screening and identification of severe acute respiratory syndrome-associated coronavirus-specific CTL epitopes. J Immunol 2006;177(4):2138–45.
[34] Chentoufi AA, Zhang X, Lamberth K, Dasgupta G, Bettahi I, Nguyen A, et al. HLA-A*0201-restricted CD8+ cytotoxic T lymphocyte epitopes identified from herpes simplex virus glycoprotein D. J Immunol 2008;180:426–37.
[35] Milicic A, Price DA, Zimbwa P, Booth BL, Brown HL, Easterbrook PJ, et al. CD8+ T cell epitope-flanking mutations disrupt proteasomal processing of HIV-1 Nef. J Immunol 2005;175:4618–26.
[36] Le Gall S, Stamegna P, Walker BD. Portable flanking sequences modulate CTL epitope processing. J Clin Invest 2007;117:3563–75.
[37] Barouch DH, Nabel GJ. Adenovirus vector-based vaccines for human immunodeficiency virus type 1. Hum Gene Ther 2005;16(2):149–56.
[38] Tatsis N, Ertl HC. Adenovirus as vaccine vectors. Mol Ther 2004;10(4):616–29.
[39] Wedemeyer H, Gagneten S, Davis A, Bartenschlager R, Feinstone S, Rehermann B. Oral immunization with HCV-NS3-transformed *Salmonella*: induction of HCV-specific CTL in a transgenic mouse mode. Gastroenterology 2001;121(5):1158–66.
[40] Tsao YP, Lin JY, Jan JT, Leng CH, Chu CC, Yang YC, et al. HLA-A*0201 T-cell epitopes in severe acute respiratory syndrome (SARS) coronavirus nucleocapsid and spike proteins. Biochem Biophys Res Commun 2006;344(1):63–71.
[41] BenMohamed L, Krishnan RA, Auge C, Primus JF, Diamond DJ. Intranasal administration of a synthetic lipopeptide without adjuvant induces systemic immune responses. Immunology 2002;106:113–21.
[42] Zhu X, Ramos TV, Gras-Masse H, Kaplan BE, BenMohamed L. Lipopeptide epitopes extended by an N^{ε}-palmitoyllysine moiety increase uptake and maturation of dendritic cells through a Toll-like receptor-2 pathway and trigger a Th1-dependent protective immunity. Eur J Immunol 2004;34:3102–14.
[43] Zhang X, Chentoufi AA, Dasgupta G, Nesburn AB, Wu M, Zhu X, et al. A genital tract peptide epitope vaccine targeting TLR-2 efficiently induces local and systemic CD8+ T cells and protects against herpes simplex virus type 2 challenge. Mucosal Immunol 2009;2:129–43.
[44] Davila E, Kennedy R, Celis E. Generation of antitumor immunity by cytotoxic T lymphocyte epitope peptide vaccination, CpG-oligodeoxynucleotide adjuvant, and CTLA-4 blockade. Cancer Res 2003;63:3281–8.

Biochemical and Biophysical Research Communications 391 (2010) 1494–1499

Contents lists available at ScienceDirect

Biochemical and Biophysical Research Communications

journal homepage: www.elsevier.com/locate/ybbrc

A CTL-based liposomal vaccine capable of inducing protection against heterosubtypic influenza viruses in HLA-A*0201 transgenic mice

Masanori Matsui [a], Shunsuke Kohyama [a], Tatsuya Suda [a], Shoichi Yokoyama [b], Masahito Mori [b], Akiharu Kobayashi [b], Maiko Taneichi [c], Tetsuya Uchida [c,*]

[a] Department of Microbiology, Faculty of Medicine, Saitama Medical University, Saitama, Japan
[b] Drug Delivery System Development Division, NOF Corporation, Tokyo, Japan
[c] Department of Safety Research on Blood and Biological Products, National Institute of Infectious Diseases, Tokyo, Japan

ARTICLE INFO

Article history:
Received 2 December 2009

Keywords:
Influenza
Vaccine
Liposome
CTL

ABSTRACT

The current vaccination strategy against influenza is to induce the production of antibodies directed against surface antigens of viruses. However, the frequent changes in the surface antigens of influenza viruses allow the viruses to avoid antibody-mediated immunity. On the other hand, it is known that cytotoxic T-lymphocyte (CTL) populations directed against internal antigens of influenza A virus are broadly cross-reactive to influenza virus subtypes. In the present study, liposomal conjugates with CTL epitope peptides derived from highly conserved internal antigens of influenza viruses were evaluated for their ability to protect against infection with influenza viruses. Liposomal conjugates with peptide M1 58-66, an HLA-A*0201-binding CTL epitope present within the amino-acid sequence of the M1 coding region, successfully induced antigen-specific $CD8^+$ T-cells and CTLs in HLA-A*0201-transgenic mice. Moreover, after nasal infection with either the H1N1 or H3N2 virus, viral replication in the lung was significantly inhibited in the immunized mice. These protective activities lasted at least 6 months after the immunization. Thus, these results suggest that liposome-coupled CTL epitope peptides derived from highly conserved internal antigens of influenza viruses might be applicable to the development of vaccines that induce protection against infection with heterosubtypic influenza viruses.

Introduction

A novel swine-origin influenza A (H1N1) virus (S-OIV) emerged in Mexico in March 2009 and continues to spread globally via human-to-human contact. Although S-OIV belongs to the same hemagglutinin (HA) serotype as seasonal human influenza A (H1N1) viruses, vaccination with seasonal influenza vaccine does not result in cross-reactive antibodies [1], possibly because the protein sequence divergence of the S-OIV H1 from human seasonal influenza H1 is wide: around 20–24% [2]. The current vaccination strategy is to elicit neutralizing antibody responses against HA, a surface glycoprotein of influenza viruses. Although antibody-mediated immunity to the surfaces of viruses reduces the probability of infection and morbidity, an antibody against one influenza virus type or subtype can provide limited or no protection against another. Moreover, an antibody to one antigenic variant of an influenza virus might not protect against a new antigenic variant of the same type or subtype, as a consequence of the frequent development of antigenic variants through antigenic drift. Therefore, although vaccines designed to induce antibodies against HA provide reasonable protection against the homologous viruses, it is feared that the vaccines currently being produced may have HA sequences so different from those of any pandemic strain that the vaccines would have little or no efficacy, due to the high rate of viral diversification [3].

Upon natural infection, it is known that the host responds by inducing humoral and cellular immunity against the pathogen. Humoral immune responses are represented by the production of antibodies that bind to the surfaces of bacteria and viruses, whereas cellular immune responses mediate immunity to intracellular pathogens. Since Effros et al. [4] reported in 1977 that influenza A virus-specific cytotoxic T-lymphocytes (CTLs) are broadly cross-reactive for cells of the same MHC class I type infected with serologically distinct H1N1 and H3N2 viruses, it has been known that cytotoxic T-cells specific to internal proteins show high cross-reactivity between strains and between subtypes, reflecting more than 90% conservation of the internal proteins [5]. Lee et al. [6] recently reported that memory T-cells established by seasonal human influenza A infection cross-react with H5N1 in healthy individuals who have not been exposed to H5N1 viruses. $CD8^+$ T-cells of the participants recognized multiple synthesized

* Corresponding author. Address: Department of Safety Research on Blood and Biological Products, National Institute of Infectious Diseases, 4-7-1 Gakuen, Musashimurayama-city, Tokyo 208-0011, Japan. Fax: +81 42 562 7875.
E-mail address: tuchida@nih.go.jp (T. Uchida).

0006-291X/$ - see front matter © 2009 Elsevier Inc. All rights reserved.
doi:10.1016/j.bbrc.2009.12.100

influenza peptides, including peptides from the H5N1 strain. Thus, vaccine formulas that include heterosubtypic T-cell-mediated immunity might confer broad protection against avian and human influenza A viruses.

In general, extracellular antigens are presented via MHC class II molecules to $CD4^+$ T-cells, whereas intracellular antigens are presented via MHC class I molecules to $CD8^+$ T-cells. To induce influenza-specific CTLs, vaccine antigens must be loaded onto the class I MHC processing pathway in the antigen-presenting cells (APCs) via cross-presentation. In the cross-presentation, exogenous proteins cross over to the endogenous pathway to gain access to MHC class I molecules [7]. However, the currently approved alum adjuvant, which was first described by Glenny and Pope [8] in 1926, is known to be effective only for the induction of humoral immunity, not for the induction of cell-mediated immunity [9]. Consequently, the development of a novel vaccine adjuvant is essential for the production of the $CD8^+$ T-cell vaccine.

In our previous study [10], we produced surface-coupled liposomal antigens that were presented by APCs to $CD8^+$ T-cells via MHC class I molecules. Therefore, this antigen preparation was expected to be applicable to the development of viral vaccines to induce virus-specific CTLs that effectively eliminate virus-infected cells [11]. Since the liposomal conjugates induced CTLs efficiently when CTL epitope peptides were coupled to the surfaces of liposomes [10], the liposomal conjugates were expected to be applicable to the development of peptide vaccines. We recently demonstrated that liposome-coupled peptide $NP_{366-374}$, derived from nucleoprotein (NP) of influenza H3N2 viruses, induced antigen-specific CTLs and successfully suppressed influenza H3N2 viral replication in the lung in C57BL/6 mice [12]. In the present study, we evaluated a possible application of liposome-coupled peptides to the development of an influenza vaccine using HLA-A*0201-restricted CTL epitope peptides and HLA-A*0201-transgenic mice.

Materials and methods

Mice. Mice express a transgenic HLA-A*0201 monochain, designated as HHD, in which human b2-microglobulin (b2m) is covalently linked to a chimeric heavy chain composed of HLA-A*0201 (a1 and a2 domains) and $H\text{-}2D^b$ (a3, transmembrane, and cytoplasmic domains) [13]. Eight- to twelve-week-old mice were used for all experiments. The mice were housed in appropriate animal care facilities at Saitama Medical University, Saitama, Japan. Experiments in the present study were approved (No. 214) by the Animal Research Committee of Saitama Medical School and the mice were handled according to international guidelines for experiments with animals.

Reagent. Synthetic CpG ODN (5002: TCCATGACGTTCTTGATGTT) was purchased from Hokkaido System Science (Sapporo, Japan) and was phosphorothioate-protected to avoid nuclease-dependent degradation.

Synthetic peptides. The HLA-A*0201-restricted, influenza virus matrix protein-derived peptide M1 58-66 (GILGFVFTL) [14] and two newly determined peptides—NS1 128-136 (IILKANFSV), which corresponds to residues 128–136 of the nonstructural protein 1 and PB1 410-418 (GMFNMLSTV), which corresponds to residues 410–418 of the polymerase PB1 protein—were synthesized by Operon Biotechnologies (Tokyo, Japan).

Coupling of peptides to liposomes. Liposomal conjugates with peptides derived from internal antigens of influenza virus were prepared essentially in the same way as described previously [10] using disuccinimidyl suberate (DSS). Briefly, a mixture of 10 ml of anhydrous chloroform solution containing 0.136 mM DOPE and 24 ml of TEA was added in drops to 26.6 ml of anhydrous chloroform solution containing 0.681 mM DSS and stirred for 5 h at 40 °C. The solvent was evaporated under reduced pressure, and 18 ml of a 2:1 mixture of ethyl acetate and tetrahydrofuran was added to dissolve the residue. To the solution was added 36 ml of 100 mM sodium phosphate (pH 5.5) and 90 ml of saturated NaCl aqueous solution. The mixture was, shaken for 1 min and allowed to separate. To remove undesirable materials, the upper layer was washed with the same buffer. After evaporation of the solvent, 3 ml of acetone was added to dissolve the residue. Then, 100 ml of ice-cold acetone was added in drops and kept on ice for 30 min to precipitate. Crystals were collected and dissolved in 5 ml of chloroform. After evaporation, 34.4 mg of DOPE-DSS was obtained, then 0.18 mM DOPC, 0.03 mM DOPE-DSS, 0.21 mM cholesterol, and 0.06 mM DOPG were dissolved in 10 ml of chloroform/methanol. The solvent was removed under reduced pressure and 5.8 ml of phosphate buffer (pH 7.2) was added to make a 4.8% lipid suspension. The vesicle dispersion was extruded through a 0.2 mm polycarbonate filter to adjust the liposome size. A 2 ml suspension of DSS-introduced liposome and 0.5 ml of 10 mg/ml peptide solution were mixed and stirred for 3 days at 4 °C. The liposome-coupled and -uncoupled peptides were separated using CL-4B column chromatography. The resulting PBS solution of peptide-liposome conjugates, containing approximately 0.7 mg peptides/ml, was sterile filtered and kept at 4 °C until use.

Cell line. Madin-Darby canine kidney (MDCK) cell line was obtained from the American Type Culture Collection (ATCC) (Rockville, MD) and maintained in Dulbecco's modified Eagle's medium (DMEM) (Sigma-Aldrich, St. Louis, MO) supplemented with 10% fetal calf serum (FCS) (JRH Biosciences, Lenexa, KS).

Influenza viruses. Two influenza A virus strains—H1N1 (A/PR/8/34) and H3N2 (A/Aichi/2/68)—were propagated in 10-day-old embryonated hen's eggs at 35 °C for 3 days. Egg allantoic fluid containing either virus was then harvested and stocked at −80 °C. Virus titers were determined by calculating the 50% tissue culture infectious dose ($TCID_{50}$) using MDCK cells [15]. The value of 50% mouse lethal dose (LD_{50}) of the H1N1 (A/PR/8/34) virus was determined in mice that were inoculated intranasally (i.n.) under anesthesia. The A/PR/8/34 (H1N1) virus was purchased from ATCC, and the H3N2 (A/Aichi/2/68) virus was kindly provided by Dr. Hiroshi Kida of Hokkaido University, Japan.

Immunization. Mice were subcutaneously (s.c.) immunized with 100 μl solution of the peptide-liposome conjugates in the presence of 5 μg CpG.

Intracellular cytokine staining. Intracellular cytokine staining (ICS) was performed as described previously [16]. Briefly, after one week following immunization, 2×10^6 spleen cells of immunized mice were incubated with 10 mM of the peptide M1 58-66 for 5 h at 37 °C in the presence of brefeldin A (GolgiPlug™, BD Biosciences, San Jose, CA). After Fc receptors were blocked with the rat anti-mouse CD16/CD32 mAb (Fc Block™, BD Biosciences), cells were stained with FITC-conjugated rat anti-mouse CD8α mAb (BD Biosciences) for 30 min at 4 °C. The cells were then fixed, permeabilized, and stained with phycoerythrin (PE)-conjugated rat anti-mouse interferon-gamma (IFN-γ) mAb (BD Biosciences). After the cells were washed, flow cytometric analyses were performed.

Table 1
Amino acid sequences of CTL epitopes derived from internal antigens of influenza viruses.

Virus strain	M1 58-66	NS1 128-136	PB1 410-418
H1N1 (A/PR/8/34)	GILGFVFTL	IILKANFSV	GMFNMLSTV
H3N2 (A/Aichi/2/68)	GILGFVFTL	VMLKANFSV	GMFNMLSTV
H1N1 (A/New York/4290/2009)	GILGFVFTL	IVLKANFSV	GMFNMLSTV
H5N1 (A/Hong Kong/483/97)	GILGFVFTL	IILKANFSV	GMFNMLSTV

Disagreements are underlined.

In vivo CTL assay. *In vivo* CTL assay was carried out as described previously by Suvas et al. [17]. Briefly, spleen cells from naive HHD mice were equally split into two populations. One population was pulsed with 10 mM of peptide M1 58-66 and labeled with a high concentration (2.5 μM) of carboxyfluorescein diacetate succinimidyl ester (CFSE) (Molecular Probes, Eugene, OR). The other popula-

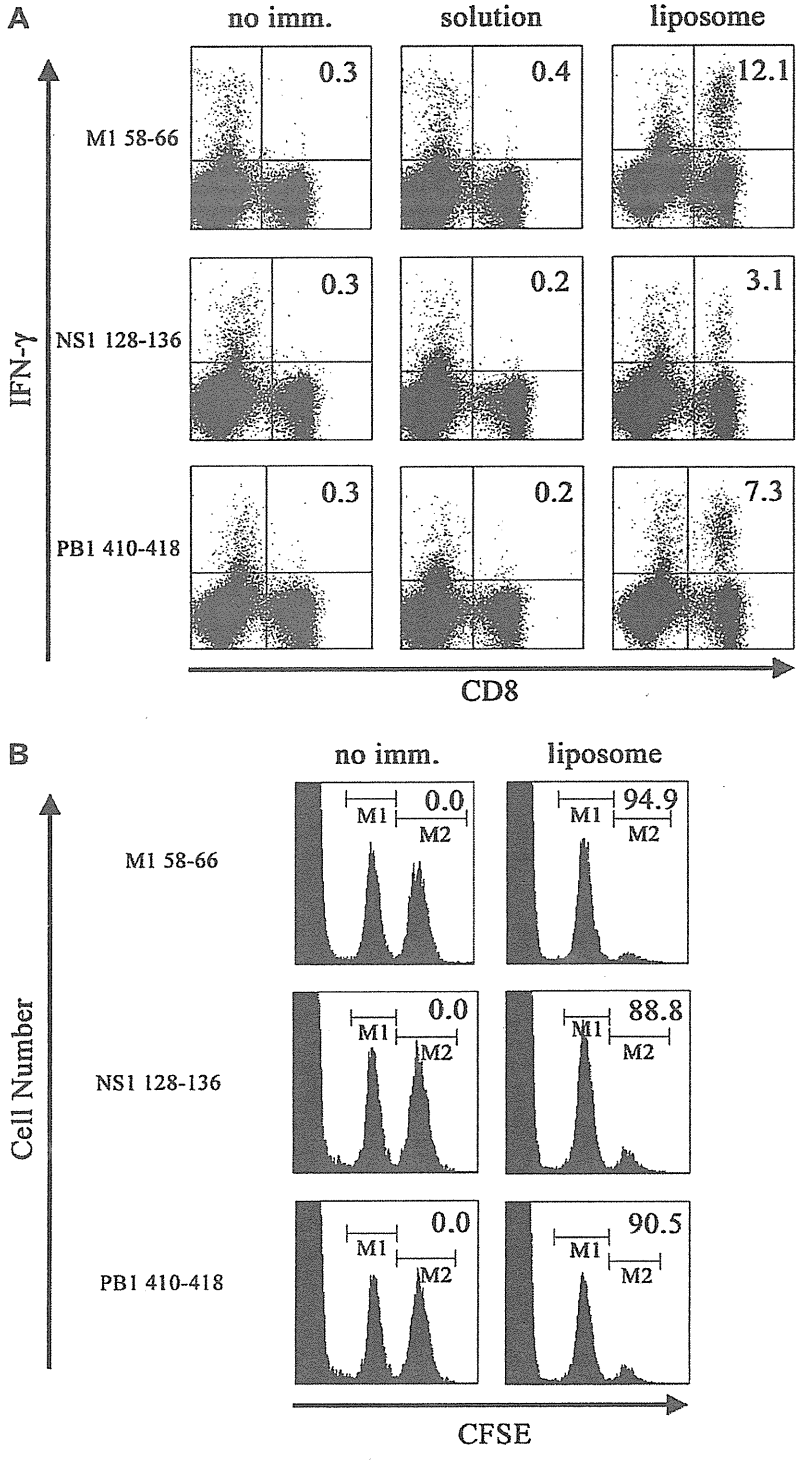

Fig. 1. Induction of antigen-specific CD8$^+$ T-cell and CTL responses. Mice received immunization with the liposome-coupled peptides M1 58-66, NS1 128-136, and PB1 410-418 (liposome) or liquefied peptides in the same amounts as liposome conjugates (solution) in the presence of CpG. Control mice received no immunization (no imm.). One week after the immunization, ICS (A) and *in vivo* CTL assay (B) were performed as described in Materials and methods. (A), ICS of antigen-specific CD8$^+$ T-cells among spleen cells of A2Tg mice. Cells were stained for their surface expression of CD8 (*x*-axis) and their intracellular expression of IFN-γ (*y*-axis). The numbers shown indicate the percentage of CD8$^+$ cells that were positive for intracellular IFN-γ. (B), induction of CTLs by liposome-coupled peptides. The numbers shown indicate the percentage of total cells killed. The data shown are representative of three independent experiments.

tion was unpulsed and labeled with a lower concentration (0.25 μM) of CFSE. An equal number (1×10^7) of cells from each population was mixed together and adoptively transferred intravenously (i.v.) into mice that had been immunized once with a liposomal peptide two weeks earlier. Twelve hours later, spleen cells were prepared and analyzed by flow cytometry. To calculate specific lysis, the following formula was used: % specific lysis = (1 − {(number of $CFSE^{low}$ cells in normal mice)/(number of $CFSE^{high}$ cells in normal mice)}/{(number of $CFSE^{low}$ cells in immunized mice)/(number of $CFSE^{high}$ cells in immunized mice)}) × 100.

Viral challenge experiment. Mice were anesthetized by an intraperitoneal injection of ketamine (175 mg/g weight) (Sigma-Aldrich) and xylazine (3.5 mg/g weight) (Bayer Holding Ltd., Tokyo, Japan), and were challenged intranasally (i.n.) with either $5 \times LD_{50}$ (1×10^4 $TCID_{50}$) of H1N1 (A/PR/8/34) virus or 1×10^4 $TCID_{50}$ of H3N2 (A/Aichi/2/68) virus resuspended in 40 ml of PBS per animal. The mice were weighed daily and monitored for mortality for two weeks. For virus titration, mice were sacrificed on day 2, 4, or 6 after the virus challenge, and the virus titers in their lungs were determined by calculating $TCID_{50}$ using MDCK cells as described [15]. In brief, the lungs were homogenized in 1 ml of PBS and the homogenate was clarified by centrifugation at 2000 rpm for 10 min. The lung homogenates were then serially 10-fold diluted in 96-well U-bottomed plates, 5 wells per dilution, starting from 10^{-1} to 10^{-7} in DMEM with 5% FCS. MDCK cells in D-5 were added to all wells (2.5×10^4 cells/well) and incubated at 35 °C in 5% CO_2. One day later, the culture medium in each well was replaced by DMEM containing 2 mg/ml acetylated trypsin (Sigma-Aldrich), and the plates were incubated in a CO_2 incubator at 35 °C for 4 more days. After the addition of 50 ml of 0.5% chicken red blood cell suspension in PBS to each well, the agglutination pattern for each sample was observed and virus titers were determined by calculating $TCID_{50}$ [15]. Three to six mice were used in each experimental group. The limit of detection in this assay was 10^3 $TCID_{50}$/mouse.

Statistical analyses. Statistical analyses were performed using Student's *t*-test. A value of $p < 0.05$ was considered statistically significant.

Results

Induction of antigen-specific CD8⁺ T-cells and CTLs by liposome-coupled CTL epitopes derived from internal proteins of influenza viruses

HLA-A*0201 (A2)-binding epitopes were predicted among the amino-acid sequences of six coding regions—M1, NP, PA, PB1, PB2, and NS—in the H1N1 influenza virus strain A/PR/8/34 (PR8) using programs available on the Internet. The predicted epitopes were then synthesized and chemically coupled to liposomes to evaluate their abilities to induce antigen-specific $CD8^+$ T-cells and CTLs by means of ICS and an *in vivo* cytotoxicity assay, respectively. Immunization of the liposome-coupled, HLA-A2-restricted epitope peptides, M1 58-66, NS1 128-136, and PB1 410-418 (Table 1), induced significant levels of antigen-specific $CD8^+$ T-cells in HLA-A2-transgenic (A2Tg) mice, as evaluated by ICS (Fig. 1A). Moreover, as shown in Fig. 1B, all the peptide-liposome conjugates in Fig. 1A induced significant *in vivo* CTL responses, indicating that all the predicted CTL epitopes were loaded onto MHC class I and were recognized by CTLs. On the other hand, solutions of the predicted peptides did not induce antigen-specific $CD8^+$ T-cells in A2Tg mice immunized even in the presence of CpG (Fig. 1A). As shown in Table 1, all three peptides were preserved well not only in H1N1 (A/PR/8/34) and H3N2 (A/Aichi/2/68) seasonal influenza viruses but also in the pandemic H1N1 2009 virus (A/New York/4290/2009) and in a highly pathogenic avian influenza virus, H5N1 (A/Hong Kong/483/97), except that NS1 128-136 partially changed in H3N2 (A/Aichi/2/68) and H1N1 (A/New York/4290/2009). Among the CTL epitopes determined in the present study, peptide M1 58-66 was already reported by Gotch et al. in 1987 [14].

Virus challenge experiment

Among the above-described HLA-A2-restricted CTL epitopes, virus challenge experiments were performed using peptide M1 58-66. A2Tg mice were immunized subcutaneously with liposome-coupled, HLA-A2-restricted peptide M1 58-66. One week after the immunization, they were infected intranasally with the influenza virus H1N1 (A/PR/8/34) or H3N2 (A/Aichi/2/68) strain. As shown in Fig. 2, viral growth in the lung was suppressed significantly in the immunized mice 2–6 days after the infection with either H1N1 (A) or H3N2 (B) viruses. Thus, immunization with liposome-coupled peptides successfully induced protection against influenza viruses regardless of the influenza virus subtypes in A2Tg mice.

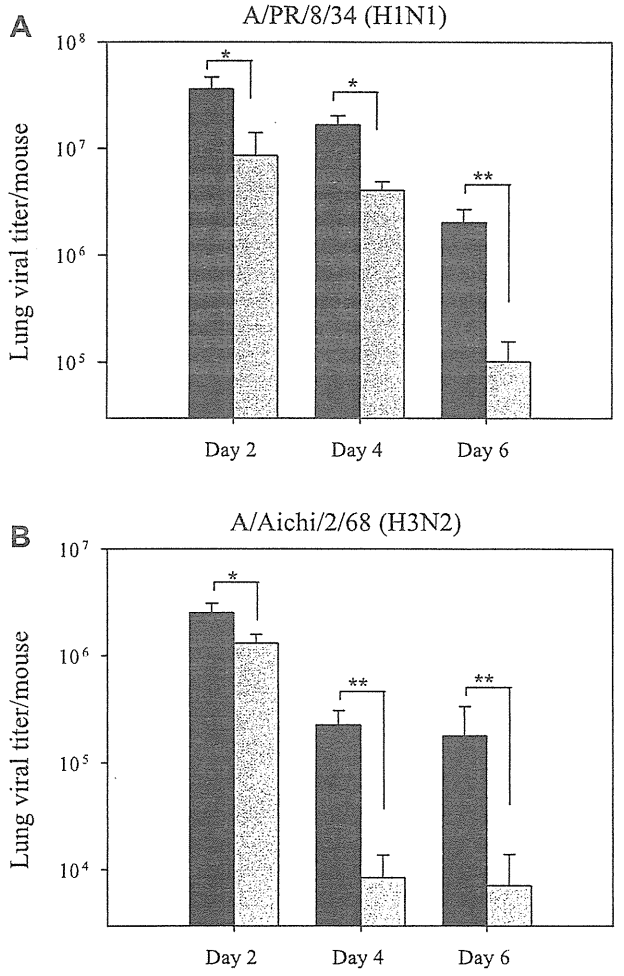

Fig. 2. Viral titers in lungs of mice following H1N1 or H3N2 virus challenge. Mice received immunization with either liposome-coupled peptide M1 58-66 liposome conjugates in the presence of CpG (gray bars) or none (black bars). One week later, mice were challenged i.n. with either the H1N1 (A) or the H3N2 virus (B). On day 2, 4, or 6 post-infection, viral titers in the lungs were determined by calculating $TCID_{50}$ using MDCK cells as described in Materials and methods. Data represent mean and SE of 5 mice per group. $^*p < 0.05$. $^{**}p < 0.01$.

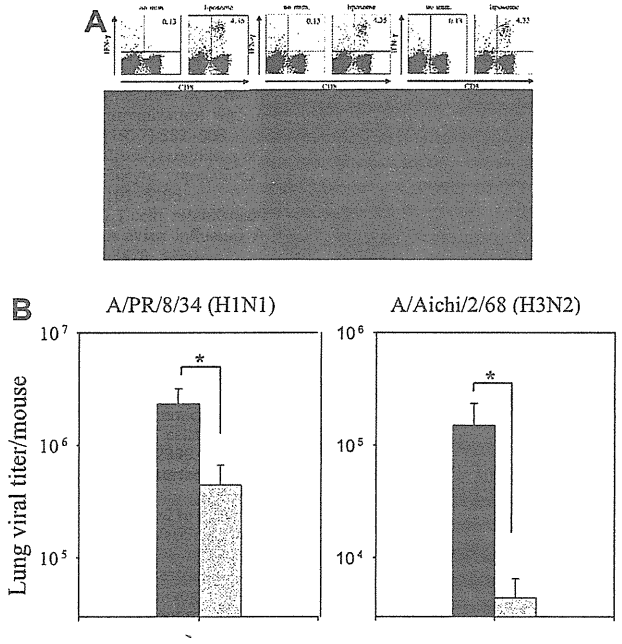

Fig. 3. Induction of long-lasting immunity by peptide-liposome conjugates. Mice were immunized with either liposome-coupled peptide M1 58-66 in the presence of CpG or none. 90 days after the immunization, ICS (A) and viral challenge experiments (B) were performed. (A), ICS of $CD8^+$ T-cells specific for peptide M1 58-66 among spleen cells of A2Tg mice immunized with liposome-coupled peptide (liposome) or none (no imm.). (B), viral replication in the lungs of mice infected with influenza viruses in mice immunized with liposome-coupled peptide (gray bars) or none (black bars). Data represent the mean and SE of 5 mice per group. $^*p < 0.05$.

Induction of memory $CD8^+$ T-cells

After confirming the induction of protective ability by liposomal peptide in the effector phase, we investigated whether or not this immunization induced memory $CD8^+$ T-cells. As shown in Fig. 3, $CD8^+$ T-cells specific to peptides M1 58-66 were detected significantly in immunized mice at 90 days after the immunization (Fig. 3A). In addition, viral growth in the lung was suppressed significantly after nasal challenge with either the H1N1 or H3N2 influenza virus (Fig. 3B). Thus, it was demonstrated that the immunization readily induced memory $CD8^+$ T-cells.

Induction of long-lasting protection against lethal doses of influenza viruses

We next investigated whether or not the long-lasting immunity demonstrated above would help protect mice against infection with lethal doses of influenza viruses. Six months after the immunization with liposome-coupled M1 58-66 peptides, mice were challenged with a lethal dose of influenza virus H1N1 PR8 strain. As shown in Fig. 4, although the immunized mice lost body weight up to 8 days after infection, the rate of loss was significantly lower than that in a non-immunized control group at 4–7 days, and the immunized mice recovered body weight thereafter (Fig. 4A). Finally, 5 out of 6 immunized mice stayed alive while all of the non-immunized control mice died within 7 days after infection with a significant loss of body weight and morbidity (Fig. 4B).

Discussion

The present study demonstrated that liposome-coupled CTL epitope peptides derived from internal antigens of influenza virus

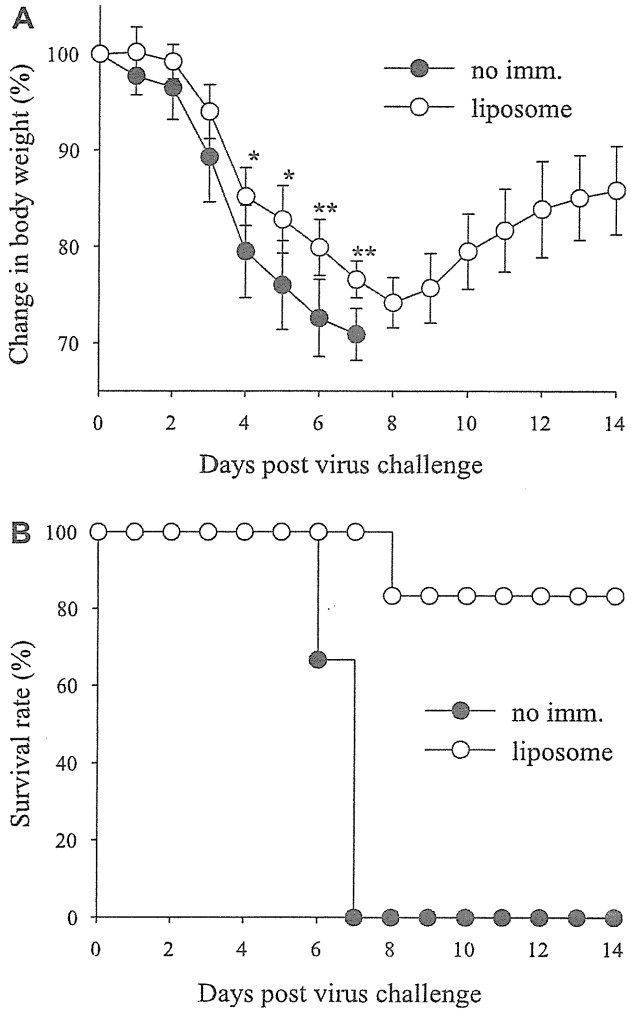

Fig. 4. Maintenance of protective ability against a lethal dose of H1N1 virus in mice immunized with liposome-coupled peptide. Mice were immunized with either liposome-coupled peptide M1 58-66 in the presence of CpG (open symbols) or none (solid symbols). Six months after the immunization, mice were challenged i.n. with $5 \times LD_{50}$ of H1N1 (A/PR/8/34) virus. The mice were weighed and monitored daily for mortality up to 14 days post-challenge. (A), changes in body weight of mice calculated as a percentage of the mean weight per group as compared with starting body weight. Data represent mean body weight and SE of 6 mice per group. $^*p < 0.05$ and $^{**}p < 0.01$ as compared with non-immunized control mice. (B), survival percentage. The mice were euthanized after they had lost 30% of their initial body weight.

protected against infection with heterosubtypic influenza viruses. Since the early finding that influenza A virus-specific CTLs are broadly cross-reactive for cells of the same MHC class I type infected with serologically distinct H1N1 and H3N2 viruses [4], numerous investigators have reported on immunodominant and cross-reactive CTL epitopes derived from conserved internal antigens, such as NP [18,19], M1 [14,19,20], and NS1 [5] of the influenza viruses. It was hoped that CTL epitopes could be used to develop a broadly protective influenza vaccine [21]. To date, candidate $CD8^+$ T-cell vaccines have been reported to induce protection even partially [22], suggesting that $CD8^+$ T-cells certainly help protect against influenza. Therefore, the $CD8^+$ T-cell vaccine strategy against influenza was expected to support antibody-focused vaccine strategies by "reducing" [21] or "dampening" [5] the impact of the next pandemic.

The liposome-coupled CTL epitope peptides efficiently induced antigen-specific $CD8^+$ T-cells and CTLs (Fig. 1), and suppressed viral

replication in the lungs of mice infected with either H1N1 or H3N2 influenza viruses (Fig. 2). In addition, since a single immunization just one week before infection successfully reduced viral replication in the lung, this vaccination protocol would be expected to counter the rapid spread of an influenza pandemic. The efficacy of the liposome-coupled peptides in inducing CTL-based protective immunity was likely due to the characteristics of liposome-coupled antigens, which are very readily recognized by APCs [23] and which effectively induce cross-presentation via MHC class I in the APCs [10], in addition to their safety, in that they are least likely to induce allergic responses [24]. Moreover, the liposome-coupled CTL epitope peptides were capable of inducing long-lived $CD8^+$ memory T-cells without including $CD4^+$ T-cell epitope in the composition of the vaccine (Fig. 3). In fact, mice immunized with liposome-coupled M1 58-66 peptides remained protected for at least 6 months after immunization (Fig. 4).

The CTL epitopes employed in the present study are contained not only in the seasonal influenza viruses but also in the currently emerging S-OIV and in the extremely virulent avian H5N1 influenza viruses (Table 1), suggesting that this liposomal peptide vaccine might be effective for protection against infection with both seasonal and pandemic influenza viruses. In addition, the liposome employed in the present study was originally developed as an antigenic carrier that effectively induces humoral immunity (i.e., antibody production) against liposome-coupled antigens [25]. Therefore, the antigen-liposome conjugates are capable of inducing both humoral and cellular immunity against influenza viruses, by combined coupling of antibody and CTL epitopes to the surfaces of liposomes.

Conclusions

The results obtained in the present study demonstrated that liposome-coupled CTL epitope peptides derived from highly conserved internal antigens of influenza viruses might be applicable to the development of a broadly protective influenza vaccine that could confer protective immunity against both seasonal and pandemic influenza.

Acknowledgments

This work was supported by a grant from The Ministry of Health, Labor and Welfare of Japan. The authors are grateful to Dr. Lemonier, Unité d'Immunité Cellulaire Antivirale, Département d'Immunologie, Institut Pasteur, Paris, France for providing the HHD mice used in the present study.

References

[1] CDC, Morbidity and Mortality Weekly Report, Serum cross-reactive antibody response to a novel influenza A (H1N1) virus after vaccination with seasonal influenza vaccine, MMWR 58 (2009) 521–524.
[2] D. Gatherer, The 2009 H1N1 influenza outbreak in its historical context, J. Clin. Virol. 45 (2009) 174–178.
[3] B. Olsen, V.J. Munster, A. Wallensten, et al., Global patterns of influenza A virus in wild birds, Science 312 (2006) 384–388.
[4] R.B. Effors, P.C. Doherty, W. Gerhard, et al., Generation of both cross-reactive and virus-specific T-cell populations after immunization with serologically distinct influenza A viruses, J. Exp. Med. 145 (1977) 557–568.
[5] J.H.C.M. Kreijtz, G. Mutsert, C.A. Baalen, et al., Cross-recognition of avian H5N1 influenza virus by human cytotoxic T-lymphocyte populations directed to human influenza A virus, J. Virol. 82 (2008) 5161–5166.
[6] L.Y. Lee, D.L.A. Ha, C. Simmons, et al., Memory T cells established by seasonal human influenza A infection cross-react with avian influenza A (H5N1) in healthy individuals, J. Clin. Invest. 118 (2008) 3478–3490.
[7] W.R. Heath, F.R. Carbone, Cross-presentation, dendritic cells, tolerance and immunity, Annu. Rev. Immunol. 19 (2001) 47–64.
[8] A.T. Glenny, C.G. Pope, Immunology notes. XXIII. The antigenic value of toxoid precipitated by potassium alum, J. Pathol. Bacteriol. 29 (1926) 31–40.
[9] H. Aggrebeck, J. Wantzin, I. Heon, Booster vaccination against diphtheria and tetanus in man: comparison of three different vaccine formations-III, Vaccine 14 (1996) 1265–1272.
[10] M. Taneichi, H. Ishida, K. Kajino, et al., Antigen chemically coupled to the surface of liposomes are cross-presented to $CD8^+$ T cells and induce potent antitumor immunity, J. Immunol. 177 (2006) 2324–2330.
[11] T. Uchida, M. Taneichi, Clinical application of surface-linked liposomal antigens, Mini Rev. Med. Chem. 8 (2008) 184–192.
[12] T. Nagata, T. Toyota, H. Ishigaki, et al., Peptides coupled to the surface of a kind of liposome protect infection of influenza viruses, Vaccine 25 (2007) 4914–4921.
[13] S. Pascolo, N. Bervas, J.M. Ure, et al., HLA-A2.1-restricted education and cytolytic activity of $CD8^+$ T lymphocytes from β2 microglobulin (β2m) HLA-A2.1 monochain transgenic H-$2D^b$ β2m double knockout mice, J. Exp. Med. 185 (1997) 2043–2051.
[14] F. Gotch, J. Rothbard, K. Howland, et al., Cytotoxic T lymphocytes recognize a fragment of influenza virus matrix protein in association with HLA-A2, Nature 326 (1987) 881–882.
[15] R. Cottey, C.A. Rowe, B.S. Bender, Influenza virus, in: Current Protocols in Immunology, John Wiley & Sons Inc., 2001, pp. 19.11.1–19.11.32.
[16] M. Matsui, O. Moriya, M.L. Belladonna, Adjuvant activities of novel cytokines, interleukine (IL)-23 and IL-27 for induction of hepatitis C virus-specific cytotoxic T lymphocytes in HLA-A*0201 transgenic mice, J. Virol. 78 (2004) 9093–9104.
[17] S. Suvas, U. Kumaraguru, C.D. Pack, et al., $CD4^+CD25^+$ T Cells regulate virus-specific primary and memory $CD8^+$ T cell responses, J. Exp. Med. 198 (2003) 889–901.
[18] S.L. Epstein, W. Kong, J.A. Miplon, et al., Protection against multiple influenza A subtypes by vaccination with highly conserved nucleoprotein, Vaccine 23 (2005) 5404–5410.
[19] A.R.M. Townsend, J. Rothbard, F.M. Gotch, et al., The epitopes of influenza nucleoprotein recognized by cytotoxic T lymphocytes can be defined with short synthetic peptides, Cell 44 (1986) 959–968.
[20] E.G.M. Berkhoff, D. Wit, M.M. Geelhoed-Mieras, et al., Functional constrains of influenza A virus epitopes limit escape from cytotoxic T lymphocytes, J. Virol. 79 (2005) 11239–11246.
[21] P.C. Doherty, A. Kelso, Toward a broadly protective influenza vaccine, J. Clin. Invest. 118 (2008) 3273–3275.
[22] P.G. Thomas, R. Keating, D.J. Hulse-Post, et al., Cell-mediated protection in influenza infection, Emerg. Infect. Dis. 12 (2006) 48–54.
[23] Y. Tanaka, M. Kasai, M. Taneichi, et al., Liposomes with differential lipid components exert differential adjuvanticity in antigen-liposome conjugates via differential recognition by macrophages, Bioconjug. Chem. 15 (2004) 35–40.
[24] M. Taneichi, S. Naito, H. Kato, et al., T cell-independent regulation of IgE antibody production induced by surface-linked liposomal antigen, J. Immunol. 169 (2002) 4246–4252.
[25] Y. Nakano, M. Mori, S. Nishinohara, et al., Surface-linked Liposomal antigen induces IgE-selective unresponsiveness regardless of the lipid components of liposomes, Bioconjug. Chem. 12 (2001) 391–395.

Immunogenicity of Whole-Parasite Vaccines against *Plasmodium falciparum* Involves Malarial Hemozoin and Host TLR9

Cevayir Coban,[1] Yoshikatsu Igari,[1,5] Masanori Yagi,[2] Thornik Reimer,[4] Shohei Koyama,[1] Taiki Aoshi,[2] Keiichi Ohata,[1,5] Toshihiro Tsukui,[5] Fumihiko Takeshita,[6] Kazuo Sakurai,[7] Takahisa Ikegami,[3] Atsushi Nakagawa,[3] Toshihiro Horii,[2] Gabriel Nuñez,[4] Ken J. Ishii,[1,2,*] and Shizuo Akira[1,*]
[1]Laboratory of Host Defense, WPI Immunology Frontier Research Center
[2]Department of Molecular Protozoology, Research Institute for Microbial Diseases
[3]Institute for Protein Research
Osaka University, Osaka 565-0871, Japan
[4]Department of Pathology and Comprehensive Cancer Center, The University of Michigan Medical School, Ann Arbor, MI 48109, USA
[5]ZENOAQ, Nippon Zenyaku Kogyo Co. Ltd., Fukushima 963-0196, Japan
[6]Department of Molecular Biodefense Research, Yokohama City University Graduate School of Medicine, Yokohama 236-0004, Japan
[7]Department of Chemical Processes & Environments, The University of Kitakyushu, Fukuoka 808-0135, Japan
*Correspondence: kenishii@biken.osaka-u.ac.jp (K.J.I.), sakira@biken.osaka-u.ac.jp (S.A.)
DOI 10.1016/j.chom.2009.12.003

SUMMARY

Although whole-parasite vaccine strategies for malaria infection have regained attention, their immunological mechanisms of action remain unclear. We find that immunization of mice with a crude blood stage extract of the malaria parasite *Plasmodium falciparum* elicits parasite antigen-specific immune responses via Toll-like receptor (TLR) 9 and that the malarial heme-detoxification byproduct, hemozoin (HZ), but not malarial DNA, produces a potent adjuvant effect. Malarial and synthetic (s)HZ bound TLR9 directly to induce conformational changes in the receptor. The adjuvant effect of sHZ depended on its method of synthesis and particle size. Although natural HZ acts as a TLR9 ligand, the adjuvant effects of synthetic HZ are independent of TLR9 or the NLRP3-inflammasome but are dependent on MyD88. The adjuvant function of sHZ was further validated in a canine antiallergen vaccine model. Thus, HZ can influence adaptive immune responses to malaria infection and may have therapeutic value in vaccine adjuvant development.

INTRODUCTION

Whole-microbe vaccines have been successful in preventing and/or treating many infectious diseases, by harboring not only protective antigens, but also "built-in" adjuvant components capable of activating the innate immune system (Pulendran and Ahmed, 2006; Ishii et al., 2008; Palm and Medzhitov, 2009). In the case of malaria, there is evidence that host protective immunity against blood stage malaria parasites can be achieved in humans as well as in animal models following whole-parasite vaccinations, although large numbers of parasites are required (Good, 2009; Doolan et al., 2009). Among parasite-derived molecules, potentially protective antigens have been investigated intensively for vaccine development (Girard et al., 2007; Coppel, 2009). However, the adjuvant components within blood stage parasites have not been explored; likely adjuvant components include ligands for innate immune receptors, such as Toll-like receptors (TLRs), NOD-like receptors (NLRs), and RIG-I-like receptors (Stevenson and Riley, 2004; Coban et al., 2007a).

There are several candidate molecules in Plasmodium parasites that could act as adjuvant components (Schofield et al., 2002; Pichyangkul et al., 2004; Krishnegowda et al., 2005; Coban et al., 2005; Parroche et al., 2007; Seixas et al., 2009). TLR2 and TLR9 have been shown to mediate innate immune system activation by GPI, a heat-labile fraction, and hemozoin (HZ) and DNA derived from *Plasmodium falciparum* (*Pf*) (Krishnegowda et al., 2005; Pichyangkul et al., 2004; Coban et al., 2005; Parroche et al., 2007); however, discrepancies among these findings remain unresolved (Coban et al., 2007a). TLR9 has also been proposed to play important roles in the pathogenesis of cerebral malaria by recruiting immune cells into the brain (Coban et al., 2007b; Griffith et al., 2007), or in that of severe malaria owing to the induction of regulatory T cells and/or synergy with interferon γ (IFNγ) signaling (Hisaeda et al., 2008; Franklin et al., 2009), but this is also controversial with some reports suggesting that this is not the case (Lepenies et al., 2008; Togbe et al., 2007). In addition, recent reports suggest that uric acid is released during malaria infection (Orengo et al., 2008), thereby activating the innate immune system presumably via NLRs, particularly NLRP3 (also known as NALP3) and its adaptor molecule apoptosis-associated speck-like protein containing a CARD domain (ASC), leading to caspase-1 activation (Franchi et al., 2009).

We therefore investigated further whether TLRs, and TLR9 in particular, as well as other innate immune receptors such as NLRs, are involved in *Pf*-mediated innate and adaptive immune responses, and whether HZ plays any role in such adaptive immune responses. We found that *Pf* whole-parasite crude

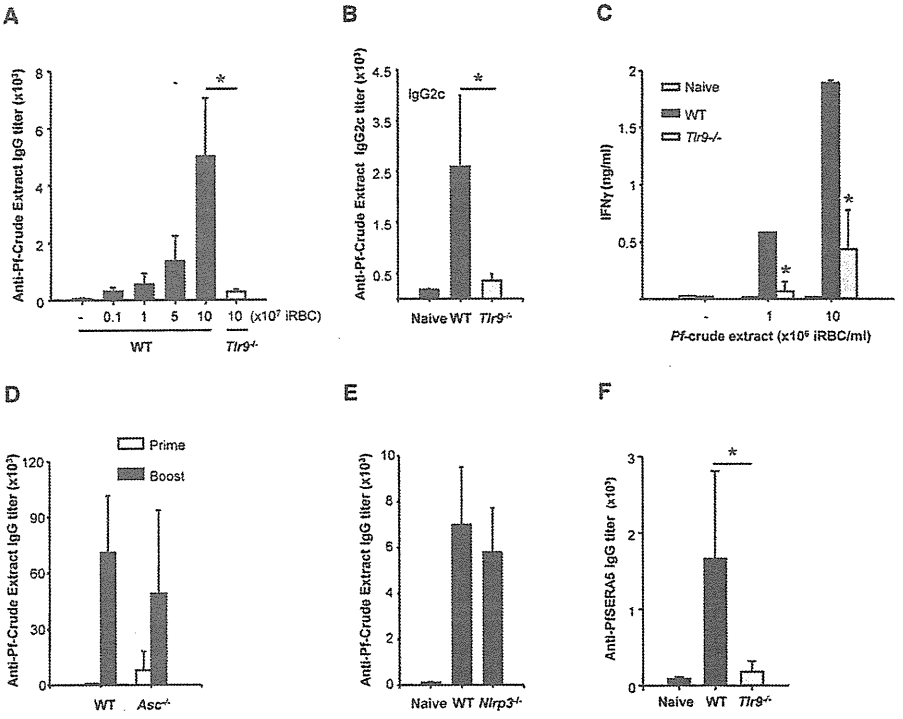

Figure 1. *Pf* Crude Extract Contains an Adjuvant Element for Coadministered Malaria Antigens in a TLR9-Dependent Manner

(A–C) Serum anti-*Pf* crude extract-specific IgG (A) and IgG2c antibody responses (B) and IFNγ from cultured spleen cells (C) were measured by ELISA at 3 weeks after the intraperitoneal immunizations with *Pf* crude extract. See also Figure S1.

(D and E) Serum anti-*Pf* crude extract-IgG antibody responses of *Nlrp3*$^{-/-}$ and *Asc*$^{-/-}$ mice. (E) shows levels only after prime immunization.

(F) Sera from WT and *Tlr9*$^{-/-}$ mice were analyzed for anti-*Pf* SERA5-specific IgG responses. The results shown are representative of at least two independent experiments with three to five mice per group. (*$p < 0.05$; mean levels of serum antibodies ± standard deviation [SD]).

extracts elicit parasite antigen-specific adaptive immune responses via TLR9, but not via NLRP3 or ASC. The malarial product HZ showed a potent adjuvant effect without any requirement for DNA. Further analysis at the molecular and atomic levels revealed that TLR9 binds to HZ directly and specifically, in a manner that depends on particular motifs and amino acid sequences, similar to its binding of CpG DNA, a well-known TLR9 ligand. A synthetic version of HZ also displayed a strong adjuvant effect; however, its optimal response was quite variable and dependent on its method of synthesis as well as its structural appearance.

RESULTS

A *Pf* Crude Extract Contains a TLR9 Ligand as a Built-in Adjuvant for Coadministered Malaria Antigens

To examine the possible adjuvant effects of whole parasites, we prepared a large quantity of whole-parasite antigens by freeze-thawing of *Pf*-infected red blood cells. The resulting extract, designated the *Pf* crude extract, contained products from both parasites and host red blood cells was immunized into mice. Three weeks after immunization, without any additional adjuvant, a significantly higher titer of serum *Pf* crude extract-specific immunoglobin G (IgG) was detected compared with the titers in naive mice and mice immunized with a normal red blood cell extract, in a dose-dependent manner (Figure 1A and data not shown). The antibody titers were 10 times higher after boost immunizations (Figure 1D).

We subsequently examined whether the immunogenicity of the whole-parasite vaccine was altered in the absence of TLR9, because TLR9 has been shown to mediate innate immune system activation by a heat-labile fraction, HZ and DNA derived from *Pf* (Coban et al., 2007a). Accordingly, mice lacking TLR9 showed significantly lower serum IgG (mainly IgG2c) responses and T-cell-specific IFNγ levels than wild-type mice (Figures 1A–1C). This TLR9-dependent adjuvant effect of whole-parasite antigens was specific for the immunizing *Pf* antigens, such as *Pf* SERA5 and *Pf* MSP1 (Figure 1F and data not shown). TLR9-dependent IgG responses were also observed for IgG2b and IgG3, but not for IgG1 (see Figures S1A–S1C available online). These data clearly demonstrate that *Pf* crude extract possesses a TLR9 ligand as a built-in adjuvant for coadministered malaria antigens.

The ASC-Inflammasome Is Not Involved in the Adjuvant Effect of *Pf* Crude Extract

We next investigated whether the inflammasome and its components were involved, given the fact that *Plasmodium* parasites grown in erythrocytes increase the concentration of uric acid, a known NLRP3 ligand that acts as a "danger signal" and

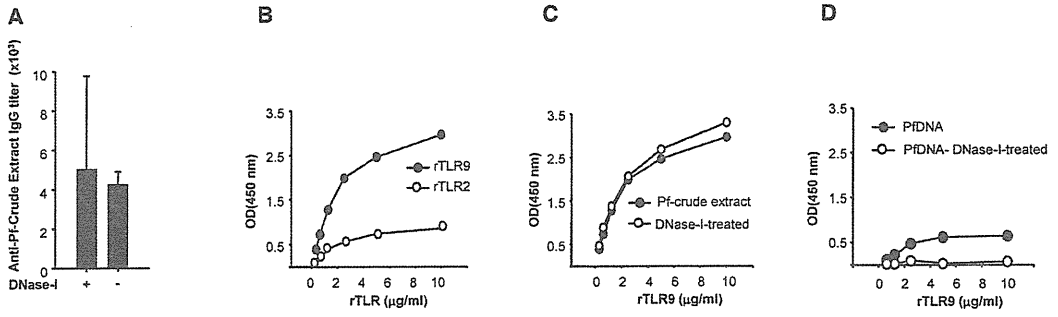

Figure 2. Malarial DNA Has No Role in the Adjuvanticity of *Pf* Crude Extract

(A) Serum anti-*Pf* crude extract-specific IgG antibody responses after immunization with DNase-I-treated and DNase-I-untreated *Pf* crude extracts. (n = 5 mice per group; mean ± SD). See also Figure S2B.

(B) Specific binding of rTLR2 or rTLR9 proteins to the coated *Pf* crude extract measured by ELISA. See also Figure S2A.

(C and D) Specific binding of rTLR9 protein to the coated DNase-I-treated or DNase-I-untreated *Pf* crude extract (C), or, to *Pf* DNA or DNase-I-treated *Pf* DNA (D). See also Figure S2B.

activates the ASC-inflammasome (Orengo et al., 2008). Moreover, recent studies suggest that DNA from any living organism may activate the ASC-inflammasome, independently of TLR9 (Muruve et al., 2008; Takeshita and Ishii, 2008), and that this may be mediated by AIM2 (Roberts et al., 2009; Hornung et al., 2009; Fernandes-Alnemri et al., 2009; Burckstummer et al., 2009). However, neither ASC- nor NLRP3-deficient mice showed any reduction in the adjuvant effect of *Pf* crude extract (Figures 1D and 1E). These data suggest that the critical adjuvant activity within *Pf* crude extract is mediated by TLR9, but not ASC-inflammasome.

Pf DNA Is Not Involved in the Adjuvant Effect of *Pf* Crude Extract

What components of the malaria parasite are responsible for the TLR9-dependent adjuvant effect? Although immune recognition of malarial HZ by TLR9 has been previously demonstrated in vitro and in vivo (Coban et al., 2005), another study suggested that HZ itself was immunologically inert, and that TLR9-dependent immune activation is instead caused by HZ-conjugated malarial DNA (Parroche et al., 2007). To investigate whether Plasmodium DNA is responsible for the TLR9-dependent adjuvant effect of *Pf* crude extract, DNA was removed by DNase-I treatment. To confirm that DNA was successfully removed from *Pf* crude extract, we performed *Pf* typing polymerase chain reaction (PCR) based on the nested PCR technique (Snounou et al., 1993), and did not find a trace of *Pf*DNA after DNase-treatment (Figure S2B). After immunizations, we found that the TLR9-dependent adjuvant effect of whole-parasite antigens was not affected by DNase-I treatment (Figure 2A), suggesting that DNA is not the TLR9-dependent adjuvant component of *Pf* crude extract.

A ligand is defined as a molecule with affinity and specificity for binding directly to a receptor. To examine such direct interactions between TLR9 and *Pf* crude extract, we established an enzyme-linked immunosorbent assay (ELISA)-based binding assay. Both rTLR9 and rTLR2 showed specific interactions with their cognate ligands (Figure S2A), confirming previous findings (Rutz et al., 2004). When the *Pf* crude extract was tested for binding to rTLR9 and rTLR2, we found that TLR9, and to a lesser extent TLR2, interacted strongly and in a dose-dependent manner with the *Pf* crude extract (Figure 2B), consistent with the findings of a previous report (Parroche et al., 2007). However, in sharp contrast with their findings, DNase-I treatment of the *Pf* crude extract did not alter its interaction with rTLR9, while the same DNase-I treatment abrogated TLR9 binding to *Pf* genomic DNA (Figures 2C and 2D). Of note, in contrast to the findings of Parroche et al., several attempts using nuclease treatment of *Pf* crude extract with several nuclease sources, showed either no effect on *Pf* crude extract binding to TLR9 or even nonspecific binding to TLR9 protein (Figures S2B and data not shown). Taken together, these data clearly demonstrate that some component of the *Pf* crude extract acts as a TLR9 ligand, mediates adaptive immune responses through TLR9, and directly binds to rTLR9 in a specific manner, and that this interaction does not require or involve DNA.

Hemozoin Binds Specifically to and Changes the Conformation of TLR9

After eliminating the possible involvement of genomic DNA in *Pf* crude extract adjuvanticity, we next investigated the role of hemozoin as a possible adjuvant molecule in the *Pf* crude extract. Given that it is not possible to deplete hemozoin from *Pf* crude extract without denaturing the malarial antigens (Figure S2C), and that using extensively purified natural *Pf*HZ would always be questioned on the basis of its purity, we used synthetic hemozoin derived from a highly pure source and thought to be identical to natural HZ (Pagola et al., 2000). Competition assays were then performed to investigate whether sHZ could block the binding of TLR9 protein to *Pf* crude extract. TLR9 binding to the coated *Pf* crude extract was measured in the presence of sHZ, CpG DNA (another known TLR9 ligand) or monosodium urate crystals (MSU). MSU crystals are insoluble immunostimulatory crystals that activate the innate immune system in a TLR9-independent manner (Martinon et al., 2006), because they form crystals that resemble sHZ in size and rod shape by surface electron microscopy (Figure S2E). TLR9 binding to the *Pf* crude extract was blocked by sHZ in a dose-dependent manner, as

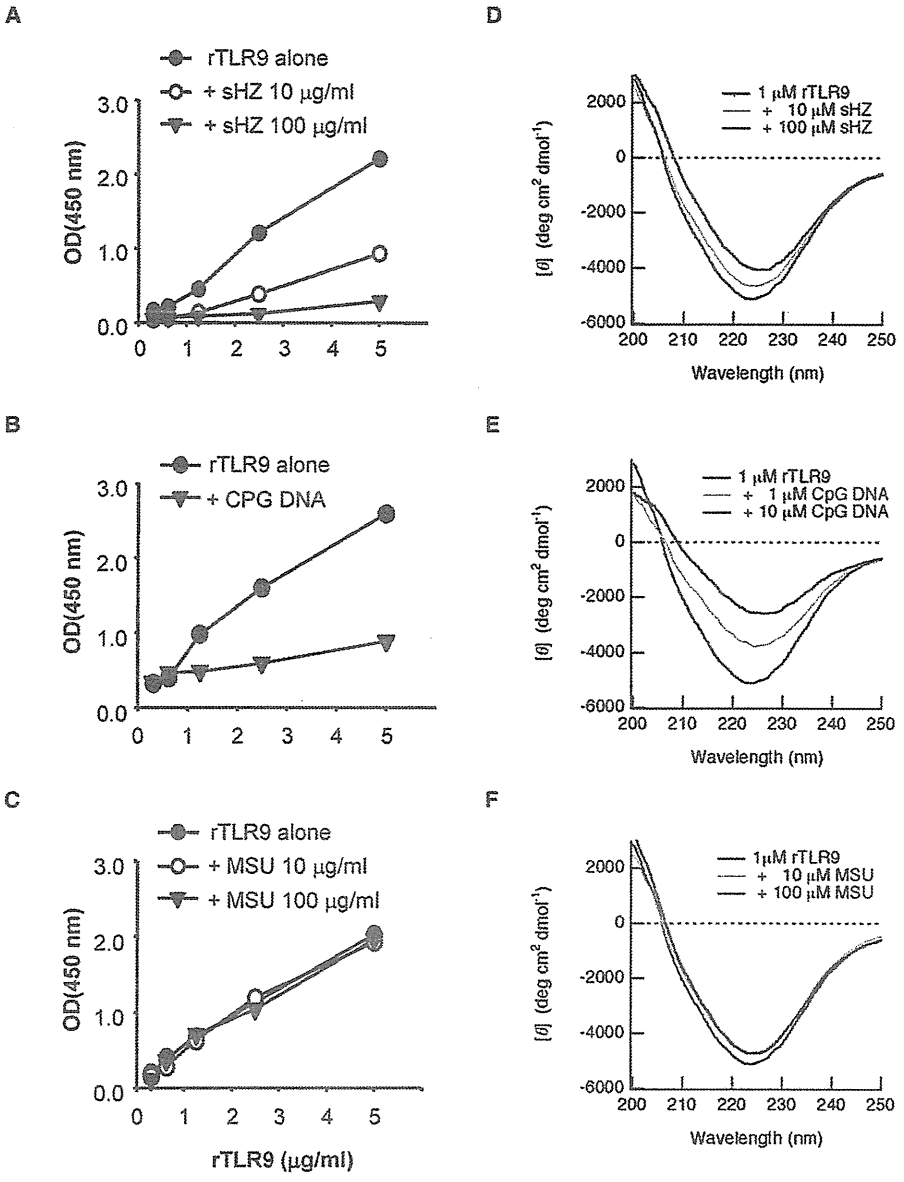

Figure 3. Synthetic Hemozoin Competes with *Pf* Crude Extract or CpG DNA for Binding to rTLR9 Protein

(A–C) Specific competition between the *Pf* crude extract and sHZ (A), CpG DNA (B) or MSU (C) was measured by ELISA.

(D–F) Conformational changes of rTLR9 protein were measured by CD in the presence and absence of sHZ (D), CpG DNA (E), or MSU (F). See also Figures S2C and S2F. All experiments were repeated at least five times with similar results.

well as CpG DNA (Figures 3A and 3B). On the other hand, MSU did not alter the binding of TLR9 to *Pf* crude extract (Figure 3C). Latz et al. recently demonstrated that TLR9 protein changes its conformation upon ligation (Latz et al., 2007). To monitor the conformational changes in the rTLR9 protein accompanying binding of its ligands, circular dichroism (CD) measurements were performed. Specifically, the CD spectra of rTLR9 protein were measured with or without the ligands at pH 5.5. The CD spectra of rTLR9 were altered by CpG DNA and sHZ, but not MSU, in a dose-dependent manner, characterized by remarkable spectral changes with shifts of the zero crossing point (Figures 3D–3F and Figure S2C). We also performed similar studies with soluble hemin that showed similar pattern and changed the conformation of rTLR9 as sHZ did, but not synthetic dsRNA (poly I:C) (Figure S2F). Taken together, these results demonstrate that sHZ can compete with *Pf* crude extract for binding to rTLR9 and change its conformation in a similar manner to CpG DNA.

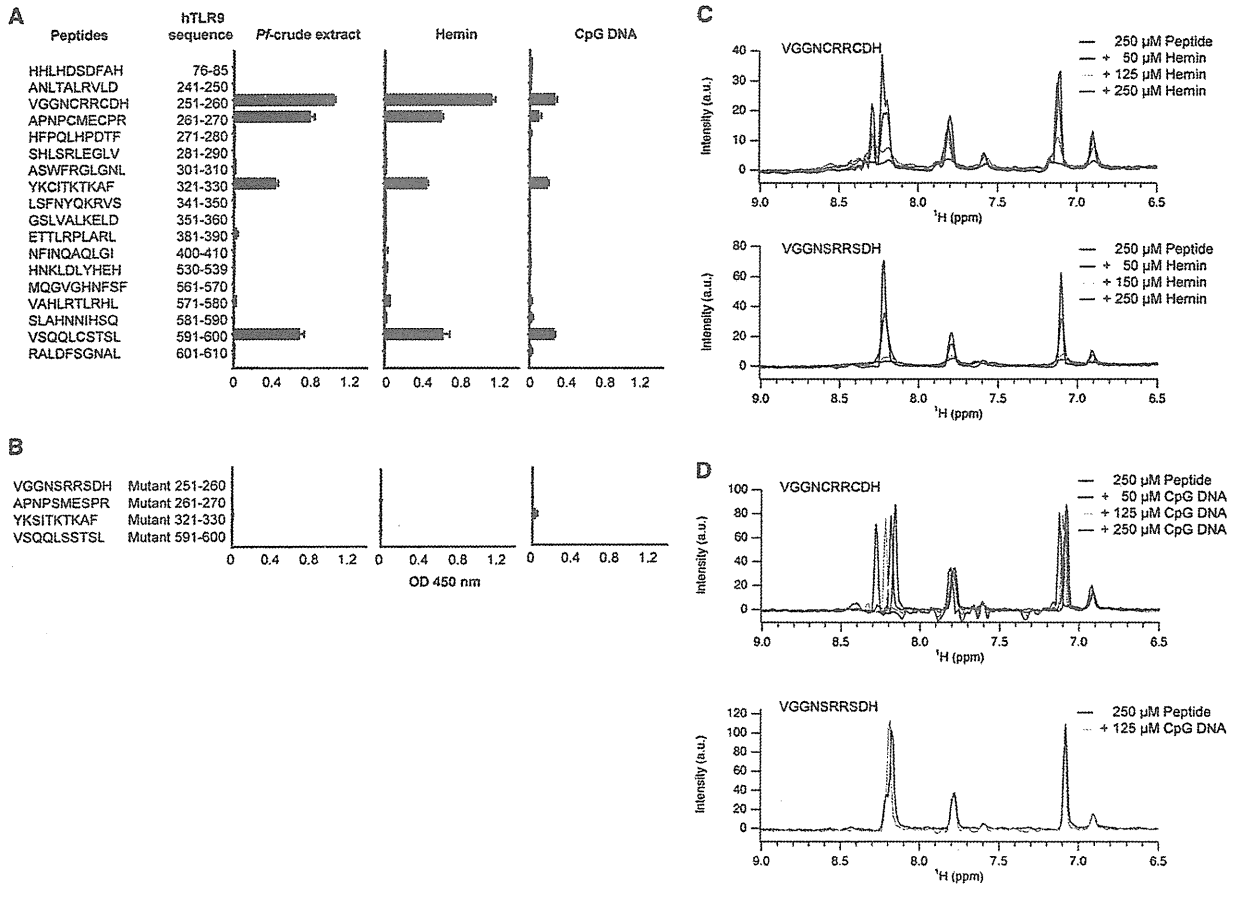

Figure 4. Peptide Regions in the Human TLR9 Sequence that Bind to *Pf* Crude Extract, Hemin, and CpG DNA

(A) Peptide sequences that are specific to human TLR9 extracellular domain and their binding to *Pf* crude extract, hemin and CpG DNA are investigated by ELISA.

(B) Binding of the peptides in which CysXXCys and Cys were respectively replaced with SerXXSer and Ser, as investigated by ELISA. Cys residues are labeled red, Ser residues are green.

(C and D) Interaction of the peptide VGGNCRRCDH and its mutant to various concentrations of hemin (C) or CpG DNA (D), as investigated by NMR titration. See also Figure S3. One-dimensional ^{1}H spectra of the peptides were obtained upon the addition of hemin or CpG DNA, and they are shown overlapped.

Direct and Specific Interaction between Hemozoin and TLR9 Observed at the Molecular and Atomic Levels

To further clarify the nature of the interaction between TLR9 and HZ, short peptides containing unique sequences of the TLR9 extracellular domain (sequences that are specific to the TLR9 extracellular domain and not contained in the extracellular domains of the other TLR family proteins) were synthesized and screened to identify the binding site(s) for TLR9 ligands. The peptides were subjected to ELISA-based binding assays with various TLR9 ligands, namely, *Pf* crude extract, hemin (a single unit of HZ) and CpG DNA (Figure 4A). Only four peptides, all of which had unique CysXXCys or Cys motifs similar to zinc finger motifs, bound to these ligands. Cysteine was required for the binding of these peptides as revealed by the same assays using mutant peptides (in which Cys was mutated to Ser) for which the binding ability was completely abrogated (Figure 4B). To analyze the binding sites in the peptides at an atomic level, nuclear magnetic resonance (NMR) titration was performed with peptides and CpG DNA and hemin. Using the peptide VGGNCRRCDH, which had the highest binding to the TLR9 ligands (Figure 4A), and its mutant peptide, the concentration of hemin and CpG DNA was increased stepwise and the spectral changes caused by hemin and CpG DNA were followed for each, as shown in Figures S3A and S3B and in greater detail in Figures 4C and 4D. Both hemin and CpG DNA shifted a peak at a ^{1}H resonance frequency of 8.2 ppm and slightly shifted at 7.1 and 7.8 ppm; all peaks were broadened to a lower intensity, upon addition of increasing concentrations of hemin, although no significant broadening was observed for CpG DNA (Figures 4C and 4D). When we performed the same titration experiments using the mutant peptides that lack Cys, we observed no such shifts (Figures 4C and 4D), although a decrease in intensity still remained upon increasing the concentration of hemin. These results indicate that TLR9 binds both HZ and CpG DNA and suggest that 4 cysteine residues may play an important role in the interaction between TLR9 and its ligands.